Investigation into a Low Cost Low Energy IoT enabled Wireless Sensor Node for Particulate Matter Prediction for Environmental Applications

by

JALPA BHARATKUMAR SHAH
201121001

A Thesis Submitted in Partial Fulfillment of the Requirements for the Degree of

DOCTOR OF PHILOSOPHY

to

Dhirubhai Ambani Institute of Information and Communication Technology

August 2019

Declaration

This is to certify that

1. The thesis comprises my original work towards the degree of Doctor of Philosophy at Dhirubhai Ambani Institute of Information and Communication Technology and has not been submitted elsewhere for a degree,

2. Due acknowledgment has been made in the text to all other material used.

Jalpa B Shah

Certificate

This is to certify that the thesis work entitled "Investigation into a Low Cost Low Energy IoT enabled Wireless Sensor Node for Particulate Matter Prediction for Environmental Applications" has been carried out by Jalpa B Shah (201121001) for the degree of Doctor of Philosophy at *Dhirubhai Ambani Institute of Information and Communication Technology* under my supervision.

Prof. Biswajit Mishra
Thesis Supervisor

Abstract

In recent years, increased transportation, removal of trees for making buildings, establishment of new industries, are the main sources of increased pollution. Increased pollution is one of the major challenge faced by all countries as it affects environment and human health. On of the way to deal with this challenge is monitoring the environment quality and taking corrective steps for the same. The conventional instruments used for environment monitoring are accurate but costly, time consuming, requires human intervention and lacking in terms of portability. Internet of Things (IoT) enabled wireless sensor node is one of the ideal solutions for real time monitoring of environment in today's urban ecosystems. We have developed a low power IoT enabled wireless sensing and monitoring platform for simultaneous monitoring, real time data of ten different environmental parameters such as Temperature, Relative Humidity, Light, Barometric Pressure, Altitude, Carbon dioxide (CO_2), Volatile Organic Compounds (VOCs), Carbon Monoxide (CO), Nitrogen Dioxide (NO_2) and Ammonia (NH_3). We have tried to achieve low power through modification in sensor node hardware architecture and developing prediction model which eliminates the need of power hungry sensor. The proposed hardware architecture for wireless sensor node helps in reducing power and number of interfacing pins required from the microcontroller. The proposed wireless sensor node architecture is also adaptable for any other applications after replacement or removal of sensors and/or modification of supply. The developed system consists of the transmitter node and the receiver node. The data received at the receiver node is monitored and recorded in an excel sheet in a personal computer (PC) through a Graphical User Interface (GUI), made in LabVIEW. An Android application has also been developed through which data is transferred from LabVIEW to a smartphone and enables IoT. The system is validated through experiments and deployment for real time monitoring. For the proposed system reliability of transmission

achieved is 97.4%. Power consumption of the sensor node is quantified which is equal to 25.67mW and can be varied by varying the sleep time or sampling time of the node. Battery life of approximately 31 months can be achieved for the measurement cycle of 60 secs. PM2.5 is one of the important pollutants for measuring air quality. Existing methods and instruments used for the measurement of PM2.5 are more laborious, not applicable for both online and offline, having response time from a few minutes to hours and lacking in terms of portability. In this work we present the correlation study of PM2.5 with other pollutants based on the data received by Central Pollution Control Board (CPCB) online station at N 23° 0' 16.6287, E 72° 35' 48.7816. Based on the correlation results, CO, NO_2, SO_2 and VOC parameters (Benzene, Toluene, Ethyl Benzene, M+P Xylene, O-Xylene) are selected as predictors for developing PM2.5 prediction model. PM2.5 prediction model is developed using Artificial Neural Network (ANN), resulting in a simple analytical equation. Since the proposed model is expressed in simple mathematical equation, it can be deployed on a wireless sensor node enabling online monitoring of PM2.5. Closeness of predicted and actual values of PM2.5 are verified through processing derived model equations using low cost processing tool (e.g. excel sheet), thereby eliminating the need for proprietary tools. The RMSE and regression coefficient of the derived model is 1.7973$\mu g/m^3$ and 0.9986 respectively. Predicted and actual values of PM2.5 are found very close to each other and variation is in the acceptable range. Derived model is recalibrated in terms of predictors and coefficients to test it, in a different city, using data of developed low power wireless sensor node. Based on the availability of the sensors on wireless sensor node, recalibration is done for the reduction of predictors to three; CO, NO_2 and VOC. For recalibrated model, results show RMSE of 7.5372 $\mu g/m^3$ and R^2 0.9708. The obtained results show the feasibility and effectiveness of the proposed approach. Improvement in these results is possible by recalibrating prediction model based on data from multiple stations at the place of deployment. Predicted model can be used for online or offline measurement. Time involved in the measurement is less compared to conventional methods, which is equal to

the processing time of the equations. To provide accurate results proposed wireless sensor node is calibrated against the standard calibrated instruments. The proposed system has advantages over conventional methods such as less costly, automated, portable, less time consuming and having higher temporal and spatial resolution.

Acknowledgments

First and above all, I praise God, for providing me this opportunity and granting me the capability to proceed successfully. Although the work described here was performed independently, I never would have been able to complete it if not for the support of many wonderful people. I would like to offer my sincere thanks to them.

I would like to express my sincere gratitude to my supervisor Prof. Biswajit Mishra, with whom I have learned immensely. I am grateful to him for patiently supervising and directing my work, fruitful discussions, providing learning opportunities on a number of occasions, and helping me throughout all the different steps of my doctoral research endeavor for the past few years.

I extend my gratitude to my research progress committee members for their valuable suggestions during research progress seminars. I am also thankful to DA-IICT for providing me the opportunity to pursue Ph.D. On a broader note, I wish to acknowledge all the professors of DA-IICT who have inspired me directly or indirectly. I would like to thank administrative and technical staff members.

My special thanks to team members of CPCB at Vadaj and Maninagar for helping me in the deployment and for gathering data. I would like to thank Ms. Meena Rajput, curator of the Shreyas Folk Art Museum and staff members for their support in deploying system in museum and performing experiments.

I am especially grateful to my parents, my better half and my in laws for their understanding of my goals, constant love and moral support. I am also thankful to all my dearest friends for their support and encouragement.

Contents

List of Figures

List of Tables

Chapter 1

Introduction

Environment quality depends on the meteorological parameters and gas pollutants. Environment monitoring is essential for protection of environment, living resources and human health. Environment pollution is of major concern as it is increasing every year and causing irreparable damage to the earth. Environment pollution categorizes mainly into air, water, soil, noise and light pollution. Indoor and outdoor air pollution both pollutes the air which people breathe. Poor quality of air causes serious health problems [1]. Environment quality can be expressed by meteorological parameters such as temperature, humidity, light, air velocity, and gas pollutants such as CO_2, CO, NO_2, sulfur dioxide (SO_2), VOCs, suspended particulate matter (SPM) and ozone (O_3). The main sources of these pollutants are industrial, residential, transportation, trading, agricultural and natural activities such as combustion of fuels, wood fire, forest fire, etc.

Besides gaseous pollutants, the atmosphere can also be polluted by particles. Particle pollution also called particulate matter or PM is a mixture of solids and liquid droplets floating in the air. They are often separated into three classifications: coarse, fine and ultrafine particles. Coarse particles have a diameter of between 2.5µm and 10µm and quickly get down by gravity or are washed out by rain. Sources for this kind of particles are crushing or grinding operations and dust stirred up by vehicles

on roads. Whereas fine particles (0.1µm to 2.5µm in diameter) and ultrafine (< 0.1µm in diameter) particles remain in the atmosphere for a longer time and affects human health. Fine particles are produced from all types of combustion, including motor vehicles, power plants, residential wood burning, forest fires, agricultural burning, and some industrial processes. Particles less than 2.5µm in diameter are referred as fine particles. PM2.5 are fine particles of 2.5µm in diameter or smaller and can only be seen through an electron microscope. PM2.5 is an air pollutant which is major concern for human health as because of small size they can directly enter into the lungs and potentially causing serious health problems [2]. Long term fine particles exposure may cause reduced lung function. PM larger than 2.5µm referred as PM10 having diameter less than 10µm. PM2.5 is generated either from primary sources such vehicles, power plants, wood burning, industrial processes, forest or grass fires and agricultural burning processes or by secondary formation from precursor emissions [2, 3] such as Sulfur Dioxide (SO_2), Nitrogen Oxides (NO_x), Volatile Organic Compounds (VOCs) and Ammonia (NH_3).

In India, CPCB is driving an ambient air quality monitoring known as National Air Quality Monitoring Programme (NAMP). NAMP network [4] consists of 683 operating stations covering 300 cities/towns in 29 states and 6 union territories of the country. Objectives of NAMP are to determine status and trends of ambient air quality, checking whether prescribed ambient air quality standards are violated, identifying non-attainment cities and developing preventive and corrective measures. To transfer the complex air quality data into information which people can understand Air Quality Index (AQI) is calculated under NAMP [5]. AQI transforms air quality data of different pollutants into a single number, nomenclature and color There are six different AQI categories, Good, Satisfactory, Moderately polluted, Poor, Very Poor, and Severe. Each of these categories is decided based on air quality data and their likely health impacts. Overall AQI is calculated only if minimum three pollutants data are available and out which one of that should be either PM2.5 or PM10, else data are considered insufficient for calculating AQI [6].

1.1 Motivation

Traditionally, air quality is measured by monitoring stations which are equipped with conventional monitoring instruments such as analyzers, samplers. Central Pollution Control Board (CPCB) stations [7] use samplers for offline stations in which for environment monitoring samples are taken at a particular interval through sampler machine and then its analysis is done in the specialized laboratory using conventional analytical instruments. This method needs special storage facility for sample, involves more analysis time, not automated and time consuming as most of the times laboratory is not nearby. Online stations of CPCB are using conventional instruments such as analyzers. These type of monitoring stations are accurate, reliable and measuring wide range of pollutants. But conventional instruments are bulkier, very costly and bigger in size. For effective air quality monitoring, place of monitoring stations plays important role as in urban areas air quality is location and human activity dependent. Changes in urban areas arrangement or human activity requires relocation or addition of new monitoring station, which is difficult or not possible because of cost. Moreover, using conventional instruments air quality data is updated hourly basis or daily basis. So, air pollution data available from the monitoring stations are having low temporal and spatial resolution. Air pollution data changes within a few meters and in few seconds depending on the activity involved and also affects human health. This phenomena can not be monitored by conventional monitoring stations because of non scalability and availability of limited data.

To increase temporal and spatial resolution for air pollution, IoT enabled Wireless Sensor Network (WSN) is one of the ideal solution [8]. WSN provides advantages over instruments in terms of portability, labour cost, and size [9]. Using low cost portable sensors, it is possible to update the air pollution information within a few minutes or seconds [10]. Feasibility of deploying larger number of sensor nodes and low cost makes WSN suitable for increasing temporal and spatial resolution.

As per the guidelines [11] provided by CPCB, PM and VOC are the

primary pollutants for indoor air quality. Other pollutants such as CO, NO_x, SO_x are considered as secondary pollutants. As per another report of CPCB [6] mentioned earlier, PM is one of the significant parameter for finding AQI for environment monitoring. Different methods and instruments used for the measurement of PM2.5 are discussed in [12], from which only a few instruments are useful for real time measurement. Existing methods of PM2.5 measurement are labour intensive, lacking in terms of portability and having response time from a few of minutes to hours. Earlier research work is done for developing indoor and outdoor environment monitoring system. But real-world applications based implementation as per the guidelines is missing. Only a few implemented systems have targeted monitoring parameters more than five for air quality measurement and included PM as a monitoring parameter.

Different components of PM2.5 are presented in Table 1.1 [3]. PM2.5 can be predicted from the precursor gases which are containing components presented in Table 1.1. Predicted model of PM2.5 provides solution for offline and online both and having less response time compared to conventional methods. Previously developed prediction model based on past data of predictand does not eliminate the need of dedicated instruments and proprietary hardware/software tools for measurement of predictand. This presents an opportunity for a simple prediction model to be developed in the form of analytical equations based on correlation of PM2.5 with other pollutants.

Table 1.1: Minimum, Maximum and Average Contribution of Major Components to PM2.5

PM2.5 Components	**Min.**	**Max.**	**Avg.**
Sulfate (secondary)	7%	47%	24%
Nitrates (secondary)	4%	37%	13%
Ammonium (secondary)	3%	20%	13%
Black Carbon (primary)	2%	22%	10%
Organic Carbon (secondary)	11%	41%	27%
Soil (primary)	2%	25%	7%
Other (primary/secondary)	0%	23%	6%

1.2 Thesis Contributions

We have developed low power IoT enabled wireless environment monitoring system. Proposed sensor node hardware provides low power operation and saves $(3n/2)$-1 pins for interfacing, where n is even number of sensors. Due to saving in interfacing pins this architecture will be useful for future expansion without the addition of extra hardware or processor. In future, addition of more sensing parameters is possible without adding processing unit. Proposed hardware for sensor node is flexible and easily adaptable for another application by modification/ replacement of the sensor and/or power supply. It can be used for indoor and outdoor environment monitoring applications. Developed system's working is verified by its deployment in indoor and outdoor environment and through calibration. Developed system helps in monitoring environment for places such as museums, smart buildings and smart cities. Developed system monitors simultaneously real time data of ten different parameters, temperature, relative humidity, light, barometric pressure, altitude, carbon dioxide (CO_2), volatile organic compounds (VOCs), carbon monoxide (CO), nitrogen dioxide (NO_2) and ammonia(NH_3). Proposed system monitors all significant parameters for the real time monitoring. Developed GUI in LabVIEW, is useful for monitoring, storing and transferring the real time data. The data is stored in excel sheet and transferred to smartphone through developed Android application and enables IoT. Reliability of data transmission achieved is 97.4%. Power consumption of the sensor node is quantified which is equal to $25.67mW$ and can be varied by varying the sleep time or sampling time of the node. Battery life of approximately 31 months can be achieved for the measurement cycle of 60 *secs*.

Study related to correlation of PM2.5 with other pollutants and cross correlation among them is done based on the data collected from CPCB online station at N 23° 0' 16.6287, E 72° 35' 48.7816. Based on correlation results, CO, NO_2, SO_2 and VOC are selected as predictors for developing PM2.5 prediction model. PM2.5 prediction model is developed using Artificial Neural Network (ANN) resulting in simple analytical equation.

The usefulness of the proposed approach is demonstrated by porting to a low cost processing tool (e.g. excel sheet), thereby eliminating the need for proprietary tools. The RMSE and regression coefficient obtained for PM2.5 prediction model is 1.7973µg/m^3 and 0.9986 respectively. Since the proposed model is expressed in simple mathematical equations, it can be deployed on a wireless sensor node enabling online monitoring of PM2.5. The derived analytical equation of prediction is also tested in a different city, Gandhinagar, after recalibrating it in terms of predictors and coefficients. Main purpose was to test the derived model in different city using data obtained from developed wireless sensor node. Due to the availability of sensors on developed wireless sensor node, recalibration was done to reduce predictors to three; CO, NO_2 and VOC. Results show RMSE of 7.5372 µg/m^3 and R^2 0.9708. The obtained results show the feasibility and effectiveness of the proposed approach. Improvement in these results is possible by recalibrating prediction model based on data from multiple stations at the place of deployment. Conventional methods used for the measurement of PM2.5 are lacking in terms of portability, size and response time. Proposed prediction model of PM2.5 is useful for online and offline measurement and also overcomes disadvantages of conventional methods used. Proposed prediction model does not require costly and bulky instruments for PM2.5 measurements except in initial phase for training and calibration as it is not based on its own past data. Implementation of derived prediction model on wireless sensor node helps in reduction of power consumption as power hungry sensor is not required.

1.3 Thesis Organization

This thesis report contains six chapters and it is organized as follow. Literature review related to indoor and outdoor environment monitoring systems is presented in Chapter 2. Chapter 3 contains the hardware and software details about the developed low power IoT enabled wireless environment monitoring system. Details and methodology related to derivation of PM2.5 prediction model in the form of analytical equations

are given in Chapter 4. The aim of Chapter 5 is to provide the details about different applications for which developed wireless sensor node's working is verified. Finally, Chapter 6 concludes the work and gives details about possible future work.

Chapter 2

Literature Review

Major areas of concern for environment monitoring are air pollution, water pollution and soil pollution. Now a days, air pollution is a growing concern for developing and non developing countries. Poor air quality not only causes risk for our own potential for survival but also that of other animals and plants. Unfortunately, air pollution is irreversible process and it is very hard or impossible to purify the air once it is polluted. Because of this very less options are available in terms of maintaining and improving air quality compared to water and soil. Many a times, purification of indoor air also causes pollution in outdoor air. One of the way to deal with air pollution is monitoring of air quality, which helps in finding concentration of air pollutants, their sources and taking corrective actions for limiting air pollution upto certain extent.

Air pollution is caused by release of harmful gases and particles in the air that harm living organism and climate. In particulate pollution PM2.5 is one of the harmful particulate for human health. PM2.5 is one of the deadliest form of air pollution as due to its small size it can penetrate deep into the lungs and blood. It is a major contributor for diseases like asthma, lung cancer, respiratory diseases and cardiovascular diseases. Most of the governments have created regulations for emissions allowed from certain type of pollution sources and for the ambient concentration of particulates due to its highly toxic health effects. In India, CPCB is driving NAMP programme

which takes care of monitoring air quality in different regions of nation and taking corrective actions for maintaining it. As per the report of CPCB [6], PM is one of the significant parameter for finding AQI for air quality monitoring.

Different methods are used for the measurement of air pollutants: toxic gases and particulates. These methods broadly can be classified as shown in Fig. 2.1. In this Chapter we present the review of the literature related to indoor and outdoor air quality monitoring systems highlighting current research status in these areas. We first review direct methods used for air quality monitoring in Section 2.1 followed by indirect methods in Section 2.2.

2.1 Direct Methods

To obtain air pollution information of a particular region, sample of air is taken followed by its measurement to find the air quality and sources of air pollution. There are two types of sampling: continuous and time averaged. In continuous sampling sampling is carried out by sensors (optical, electrochemical, semiconductor) and spectroscopic methods which gives continuous record of concentration values. The specific time averaged data can be obtained from this record of continuous data. In time averaged sampling known volume of air is sampled for given average time. Then samples are analyzed using physical, chemical and biological methods to obtain concentration values [13]. In NAMP the monitoring of pollutants is carried out for 24 hours (4-hourly sampling for gaseous pollutants and 8-hourly sampling for particulate matter) with a frequency of twice a week, to have 104 observations in a year [4]. The couple of mentioned methods are discussed here.

In direct measurement instruments such as aethalometer [14], analyzers [7], samplers [15–17] and wireless sensor nodes [18–21] are used as mentioned in Fig. 2.1.

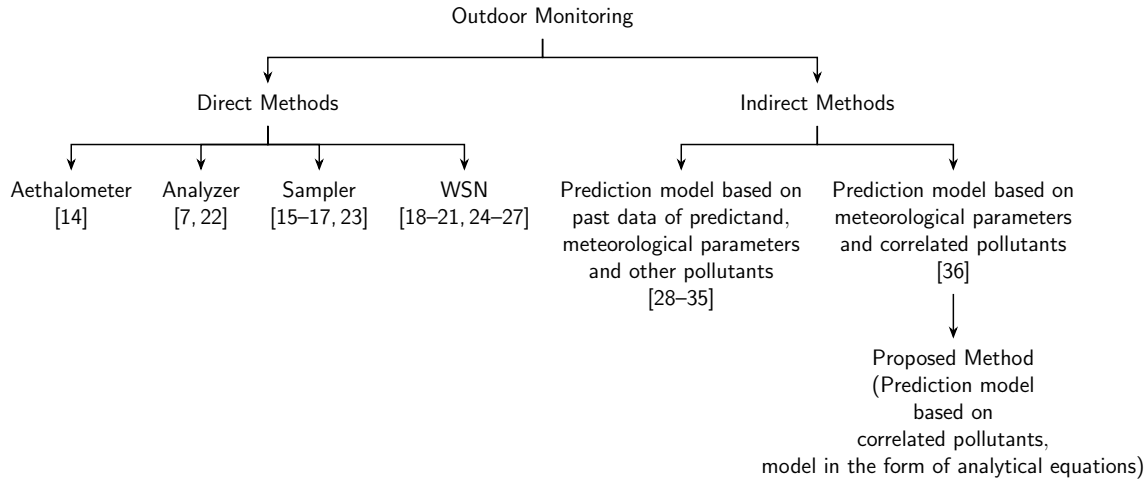

Figure 2.1: Different Methods for Outdoor Monitoring

Figure 2.2: Aethalometer

2.1.1 Aethalometer

Aethalometer [14] is mostly used for obtaining the concentration of black carbon which is the primary component of PM. Fig. 2.2 demonstrates the model of aethalometer. Aethalometer takes the air sample through inlet port at particular flow rate using internal pump. It collects the sample on filter tape on which suspended particulates are deposited. Optical analysis is performed continuously while sample is collected. Light beam of particular wavelength is passed through this deposit. The light beam is attenuated by those particle which are absorbing light and measurement is

done at successive regular time intervals. The increase in attenuation from one measurement to next is proportional to increase in density or concentration of absorbing particulates on filter. During the process, tape does not move, it will move forward when the density of deposit spot on filter reaches to a pre-set limit. Content of black carbon in sampled air can be determined from specific attenuation for particular combination of filter and optical components. This instrument is very costly and filter tape needs to be replaced after certain duration.

(a) Gas Analyzer (b) Particulate Analyzer

Figure 2.3: Analyzer

2.1.2 Analyzer

Analyzer [7] is the instrument which is capable of analyzing gases or particulates present in the sample. It gives the information about concentration of the present gases or particulates in the graphical or numerical form. Fig. 2.3 demonstrates the model of analyzer for gas and particulate. Working principle of analyzer changes depending on the target gas. Analyzers can be divided into three groups depending on their working operation: The first group includes instruments using physical methods of analysis including auxiliary chemical reactions, also known as volumetric-manometric or chemical gas analyzers. These analyzers measure

Table 2.1: Instruments Used for Monitoring Parameters at CPCB Online Station (N 23° 0' 16.6287, E 72° 35' 48.7816.)

Parameters	**Instruments**	**Measurement Method**	**Company**
CO	Carbon Monoxide Analyzer (CO12M)	Non dispersive Infrared	Environment S.A
NO,NO_2,NO_X	Nitrogen Oxides Analyzer (AC32M)	Chemiluminescence	Environment S.A
SO2	Sulfur Dioxide Analyzer (AF22M)	Ultraviolet Fluorescence	Environment S.A
O_3	Ozone Analyzer (O342M)	Ultraviolet absorption	Environment S.A
VOC	VOC Analyzer (VOC71M)	Gas Chromatography	Environment S.A
PM2.5	Particulate Matter Analyzer (MP101M)	Beta Attenuation	Environment S.A
Temperature and Humidity	Hygroclip XD	—	Rotronic

changes in pressure or volume of the gas mixture as a result of chemical reactions of its components. The second group includes instruments based on physiochemical processes such as thermochemical, electrochemical, photocolorimetric, and chromatographic. The third group is based on purely physical methods of analysis such as thermoconductometric, densimetric, magnetic, optical, and ultraviolet. Particulate analyzers are generally optical analyzers which work on the principles of scattering, absorption, and light extinction. Table 2.1 shows the detail about the instruments used for air quality monitoring by CPCB online station [22] at N 23° 0' 16.6287, E 72° 35' 48.7816. These kind of instruments use complex measurement methods and need lot of assisting tools like temperature controller, humidity controller, built in calibrator, air filter (for PM)[37]. As consequences, these instruments are very costly, power hungry, bigger in size and bulkier.

Figure 2.4: Sampler

2.1.3 Samplers

This method needs the selection of sampling method, analysis method, sampling locations, sampling frequency and sampling duration. In this type of method instruments [15–17] which takes the samples of air pollutants as shown in Fig. 2.4 are kept at particular locations known as sampling stations. These sampling stations are generally governed by objective of sampling, type of sampling and resources available. Number of sampling stations depends on the variability of the concentration of interested air pollutants. Sampling stations are generally kept at the height of 3 to 10 m

above the ground level with no direct contact of pollutant sources. Across the nation different sampling or offline stations [23] are governed by NAMP, in addition to online stations. This method is also used by offline stations of NAMP [7]. The detail procedure about sampling is discussed in [38]. Sampling tube used to preserve samples, required to be replaced manually after the sampling duration. After taking samples, sampling tubes are preserved under controlled environment and sent to the environment laboratory for analysis. In environment laboratory, analytical instruments are used for finding the concentration of the air pollutants from the sample. Majority times environment laboratory is not nearby (in different city). This method is time and human resources consuming task which leads to large delay (in days) between sample collection and receiving results.

2.1.4 WSN

The above discussed conventional monitoring instruments are having drawbacks of large size, heavy weight and extraordinary expensiveness. Majority of existing monitoring stations are using these conventional instruments for monitoring air pollution. In urban areas locations of monitoring stations are playing important role as air pollution is highly related to human activities and it is location dependent [24, 25]. Due to high cost involved for monitoring stations, it is very difficult or impossible to relocate or add new station based on the changes in the urban arrangement. Moreover, conventional monitoring instruments involve longer time duration (hourly or daily) for updating air pollution. Hence, the conventional air pollution monitoring system are having very low spatial and temporal resolutions. Limited data availability and non scalability characteristics of conventional monitoring stations will not allow them to provide detail information about air pollution which is needed for human health. Earlier research work [26, 27] show that short term acute exposure of air pollutant may trigger or worsen some health diseases.

In order to increase spatial and temporal resolutions, researchers have kept efforts in developing air pollution monitoring systems integrating low

cost portable gas sensors with WSN [18–21]. Air pollution monitoring systems based on WSN and sensors [10] can update the air pollution information in very less time (minutes or seconds). Moreover, due to low cost, portable sensors, it is possible to deploy sensor nodes in large scale. Hence, using WSN based air pollution monitoring system, it is possible to increase spatial and temporal resolution. The following part provides detail about the research work done for developing indoor and outdoor environment monitoring systems followed by comparison with the proposed IoT enabled low power wireless sensor node based environment monitoring system.

Earlier developed environment monitoring systems are either for indoor environment or for outdoor environment or for both. Different areas which are explored for indoor environment monitoring are (i) power reduction of node by reducing activity of node by means of different data processing and transmission algorithms, reducing ON time of power hungry gas sensors [39], using different routing protocols [40], different sensor censoring techniques [41] (ii) remote monitoring and controlling of system through web and smart phone [42, 43] (iii) implementation of system and its interfaces based on IEEE standards [44]. (iv) reduction of power through different power management protocols [45] and sampling techniques [46].

Environment monitoring system without wireless link was developed earlier based on IEEE standards [47]. In which the Smart Transducer Interface Module (STIM) was linked to Network Capable Application Processor (NCAP) module through Transducer Independent Interface (TII) module and all modules were developed as per IEEE 1451.2 standard guidelines. The purpose of this effort was to help in developing smart devices and interfacing those devices with instruments, systems and networks easily. In [48] neural network was used as data processing block to obtain temperature and humidity compensated accurate gas concentration values. Neural network algorithm was implemented using javascript in web server and integrated with Wireless Local Area Network (WLAN) based on adhoc architecture aimed to monitor air quality and pollution events. WSN based urban air quality monitoring system with Global System for Mobile

Communications (GSM) was deployed [49] to measure CO concentration emitted by vehicles. This work aimed to get the micro scale air quality data which can be further utilized to analyze traffic conditions and effects of it on human health. Development of low cost optical particle counter for particulate matter measurement was targeted in [50] and incorporated into WSN with other air quality monitoring sensors. Developed system was suitable to study particulate matter exposure in both indoor and outdoor environments. WSN based air pollution monitoring system was also implemented and tested [51] using zigbee protocol. Energy consumption reduction at sensor level, node level and network level was tried in [52] for indoor monitoring. Reduction in node activity is achieved by modifying node performance based on presence of people and gas concentration data from the neighbour nodes. In line with work [47], wireless STIM and NCAP were developed for environment monitoring [53] as per IEEE standards and efforts kept to achieve low cost and low energy. The power consumption of the developed system was found to be $83.6241mW$. Indoor air quality system was tested in real time environments [54], in which three different data processing algorithms were implemented for accurate sensor results and reduction in power consumption. Data smoothing algorithm helps in reducing temporary sensor errors and data aggregation algorithm helps in reducing network traffic and power consumption. But the implemented work is of hight cost and having high energy consumption. WSN based environment monitoring system based on open source Waspmote using zigbee protocol was implemented earlier [55]. In this work energy efficient routing protocol as Clustering Protocol of Air Sensor network (CPAS) was introduced, which is based on direct communication without multiple hop. Compact battery powered indoor wireless ambient monitoring system was also implemented earlier [56]. Estimated lifetime of battery for this work was three years for one transmission per hour. Calculated power consumption for the implemented system was between 42 mW and 78 mW. In earlier research work people have also tried to monitor the content of particulate matter through optical particle counter (OPC) sensor [57] with indication of hazardous situations. But it was without wireless interface. In

[58], new data aggregation algorithm named as Recursive Converging Quartiles (RCQ) was introduced for air pollution monitoring. Developed algorithm was used to merge the data so that duplicate and invalid data can be eliminated. By doing so transmitted data to sink node was reduced for energy saving. IoT cloud based data processing and analysis was also attempted [59] for air quality monitoring system built using low power wide area network and AQI was calculated based on monitored content of PM2.5 and PM10. In the proposed work AQI can be derived based on prediction data of PM2.5 and other monitored pollutants.

Summary of earlier research work and presented work is given in Table 2.2 in terms of number of parameters monitored, calibration of sensor for accuracy, type of communication, application, monitoring platform based on IoT and power consumption. In earlier research work maximum number of parameters monitored was less than ten. Only few research work estimated power consumption of the system and the presented work shows lowest power consumption of $25.67mW$. IoT is integrated with very few research work in terms of website and smart phone both.

Table 2.2: Comparison of Proposed System with Previously Developed Environment Monitoring System

parameters	**[47]**	**[48]**	**[49]**	**[50]**	**[51]**	**[52]**	**[53]**	**[54]**	**[55]**	**[56]**	**[57]**	**[58]**	**[59]**	**This work**
CO_2				X	X		X	X	X	X				X
VOC		X				X		X						X
CO	X	X	X	X		X	X	X				X		X
NO_2	X				X		X	X	X			X		X
SO_2	X				X		X	X				X		
NH_3														X
O_3	X							X	X			X		
O_2							X							
Methane		X												
GAC		X						X						
PM	X			X				X			X	X	X	
T		X	X	X			X	X		X	X		X	X
RH		X	X	X			X	X		X	X		X	X
Light										X				X
Barometric Pressure			X	X						X	X			X
Altitude														X
Calibration	X	X					X	X		X				X
Wireless		X	X	X	X	X		X	X	X		X	X	X
For Indoor		X		X		X	X	X		X	X			X
For Outdoor			X	X	X				X		X	X	X	X
Website/ smart phone		W	W						W	W			W/S	S
Power consumption		8 W		1.3W			83.62 mW	2.38 W^+		78 mW				25.67 mW

Note: + calculated based on voltage and current figures

2.2 Indirect Methods

There are many techniques available for the measurement of PM [12]. The available techniques can be grouped in to two categories: one which provides continuous measurement with sampling interval of seconds or minutes and another one which takes sample of PM and it results are analyzed manually. The second method is a gravimetric sampler based which collects PM on to a filter. This filter then weighted in to laboratory for finding concentration of PM. Due to weighting, this method is time and human resources consuming which leads to a larger delay (in days) between sample collection and obtaining results.

The commonly used continuous measurement techniques for PM are Tapered Element Oscillating Micro-Balance (TEOM) Analyzers, β-Attenuation Analyzers (BAM), Black Smoke Method and Optical Analyzers. Comparison about these techniques are given in [8]. TEOMs and BAMs are typically used in the conventional air pollution monitoring systems as having high data resolution and accuracy, large size, hight cost, heavy weight. The optical analyzers are generally small in size, light in weight, low cost and battery operated, hence widely used in hand-held monitoring devices even if having low resolution and accuracy. The majority of available sensors for PM are also based on the optical principle [60–62].

PM2.5 comes either from primary sources such as vehicles, power plants, wood burning, industrial processes, forest or grass fires and agricultural burning processes or by secondary formation from precursor emissions such as Sulfur Dioxide (SO_2), Nitrogen Oxides (NO_X), Volatile Organic Compounds (VOCs) and Ammonia (NH_3) [2, 3]. In Chapter 1, Table 1.1 lists major components [3] of PM2.5 and their minimum, maximum and average contribution. Black carbon and soil are the primary components of PM2.5. Secondary components are sulfate, nitrates, ammonium and organic carbon. Secondary components are contributed from chemical reaction of SO_2, NOx and NH_3 [3]. The sulfate aerosols concentration is related to the concentration of SO_2 and NOx [63]. The relationship between

SO_2 and sulfate [64] was investigated earlier and represented the linear relationship between both [65]. The secondary components nitrates and and ammonium are also correlated with NO_2 and NH_3 [66, 67].

As the formation of PM2.5 secondary components are related to the concentration of gas pollutants, it is possible to measure indirectly the concentration of PM2.5 based on the precursor gases concentration. Indirect methods of PM measurement eliminates the need of costly and power hungry instruments or sensors. Review about the indirect methods for the measurement of air pollution and comparison with proposed prediction model of PM2.5 are discussed in the following part of the Chapter.

The study of environmental monitoring along a subway using dedicated instruments was discussed in [14], showed the PM concentration to be higher in urban areas and need attention for healthy environment. Indirect measurement methods are divided into two categories as shown in Fig. 2.1 one in which the prediction model uses past data of the predictand itself [28–35]. In second method instead of using past data of predictand, parameters which are correlated with predictand were used as predictors [36].

Authors in [28, 29] have discussed indirect measurement methods using ANN based on the past data of O_3. In [30], a multilayer perceptron (MLP) neural network based prediction model for NO_X and NO_2 pollutants was developed based on past data of the pollutants. A hybrid approach based on autoregressive and nonlinear model for prediction of NO_2 was discussed in [31]. In [32] different models for prediction show MLP has better performance than multiple linear regression models. A neural network based prediction model for PM10 using predictors as previous day data of PM10, cloud cover, boundary layer height, wind direction and day of week was discussed in [33]. Comparison of different topologies of neural network was done for developing prediction model of PM2.5 in [34]. Hybrid approach based on box–jenkins time series or Autoregressive Integrated Moving Average (ARIMA) and ANN was discussed in [35] for prediction of PM10. Prediction of PM2.5 based on Back Propagation (BP) neural

network was explored [68] using satellite based Aerosol Optical Depth (AOD), meteorological data and past PM2.5 data. The Comprehensive Forecasting Model (CFM) was developed based on ARIMA, ANN model and Exponential Smoothing Method (ESM) [69]. Feed Forward Neural Network (FFNN) with Rolling Mechanism (RM) and Accumulated Generating Operation (AGO) of Gray model (RM-GM-FFNN) was developed [70] for prediction of PM2.5 and PM10 using past data of PM2.5 and PM10 in addition to meteorological data. Comparison of hybrid model consisting of an Ensemble Empirical Mode Decomposition and General Regression Neural Network (EEMD-GRNN), Adaptive Neuro-Fuzzy Inference System (ANFIS), Principal Component Regression (PCR), and MLR is discussed in [71] with best results obtained for EEMD-GRNN model. The research work in [72] focused on Cuckoo Search-Least Squares Support Vector Machine (CS-LSSVM) based prediction approach for PM2.5 using correlation and principal component analysis. Previous data of PM2.5 was used as a one of the predictor in addition to correlated parameters. The correlation analysis of PM2.5 to other meteorological parameters and pollutants using multivariate statistical analysis method and ANN was implemented in [73] and prediction results show RMSE of 24.06 µg/m^3 for ANN based model.

Machine learning approach in [36] have discussed the performance comparison of three supervised learning methods in Random Forests (RF), Support Vector Machines (SVMs) and ANN. The correlation study was done for five parameters in CO, NO, NO_2 and O_3 and black carbon. Furthermore, a calibration model was developed for black carbon in which meteorological parameter and other correlated pollutants were used as predictors. The RMSE of 1480.746 and R^2 of 0.586 has represented the effectiveness of the method. [74] reported better results for ANN compared to Multiple linear regression (MLR) for prediction of PM2.5 in agricultural park using PM2.5, meteorological and plant parameter data.

Previously developed prediction model based on past data of predictand, does not eliminate the need of costly instruments and proprietary software tools for measurement of predictand. This presents an opportunity of the

Table 2.3: Summary of Previously Developed Prediction Models

Reference	**Predictand**	**RMSE**	**R^2**
[28]	O_3 (ppb)	0.30	0.69
[29]	O_3 (µg/m^3)	21.78	0.73
[30]	NO_2 (ppb)	7.3	0.91
[31]	NO_2 (µg/m^3)	13.93	0.93
[32]	PM 10 (µg/m^3)	12.16	0.83
[35]	PM 10 (µg/m^3)	11.656	0.983
[68]	PM2.5 (µg/m^3)	41.97	-
[69]	PM2.5 (µg/m^3)	12.8903	-
[70]	PM10 (µg/m^3)	18.4	0.895
[70]	PM2.5 (µg/m^3)	12.7	0.954
[74]	PM2.5 (µg/m^3)	6.777	0.99
[71]	PM2.5 (µg/m^3)	5.0324	0.79
[72]	PM2.5 (µg/m^3)	14.47	-
[73]	PM2.5 (µg/m^3)	24.06	-
[36]	BC (ng/m^3)	1480.746	0.586
This Work	PM2.5 (µg/m^3)	1.7973	0.9986

prediction model to be developed in the form of a simple analytical equations based on correlation of PM2.5 with other pollutants. The proposed model presented in the form of analytical equations based on correlation results, helps in implementation of a model using low cost wireless sensor node or processing tool. The proposed model reduces the number of inputs and ANN size compared to [36]. Results related to RMSE and R^2 of previous work are shown in Table 2.3. Using the proposed approach for prediction, RMSE and R^2 is better, compared to existing methods. RMSE of 1.7973µg/m^3 and R^2 of 0.9986 is obtained for the whole range of test data set which is equal to 1838 in this case. For reduced test data set of equal to 10, RMSE obtained is 146.10 µg/m^3 and R^2 is 0.9467.

Chapter 3

Wireless Sensor Node

WSN provides advantages over customized instruments [9] in terms of portability, remote monitoring, labour cost, and size. Using low cost portable sensors, it is possible to update the air quality information in terms of AQI. Feasibility of deploying larger number of sensor nodes and low cost, makes WSN suitable for increasing temporal and spatial resolution [8]. Wireless sensor nodes operate on battery which demands low power consumption to ensure operation for longer duration.

This Chapter discusses low power environment monitoring system which monitors simultaneously real time data of ten different parameters, temperature, relative humidity, light, barometric pressure, altitude, carbon dioxide (CO_2), volatile organic compounds (VOCs), carbon monoxide (CO), nitrogen dioxide (NO_2) and ammonia(NH_3). IoT enabled monitoring platform is developed for remote monitoring of real time data of all parameters and storing them for future analysis. Validation of the proposed system is done through calibration and its deployment at different indoor and outdoor places. Proposed low power wireless sensor node is modular so it can be used for any other indoor and outdoor environment monitoring applications by replacement of sensor and/or power supply. Comparison of the proposed wireless sensor node with earlier research work shows low power consumption of sensor node with more number of monitoring parameters compared to earlier research work.

The Chapter is organized as follows. Section 3.1 provides the detail about system requirement, design parameters and architecture of the system. Results related to the deployment of the system are discussed in Section 3.2. Chapter is concluded in Section 3.3.

3.1 System Architecture

We have developed the architecture of the wireless environment monitoring system which monitors simultaneously real time data of ten different parameters. The architecture of the wireless sensing and monitoring system should have the following features, which we have tried to achieve in the proposed system.

- Energy consumption of the wireless sensor node should be as low as possible.
- Long life span of the sensors.
- System architecture should be modular so it can be used for multiple applications.
- IoT enabled monitoring platform for remote monitoring of real time data.
- High reliability of data transmission so that maximum number of data can be received at the receiver node.
- Calibration of the sensors to maintain the accuracy of the data.
- Deployment of the system in the real environment for its validation.

The proposed system block diagram [75] is shown in Fig. 3.1. Implemented system consists of one transmitter (TX) and one receiver (RX) node. Repeater nodes can be inserted between TX and RX node to expand the coverage area. RX node will transfer the received data to Personal Computer (PC) through USB interface. Developed GUI in

LabVIEW, monitors and records the data in excel sheet. Recorded data will be transferred to MySQL database vial Internet. Data from MySQL database will be further transferred to Android based smartphone via PHP API execution on Internet. Developed system architecture is flexible and adoptable for another indoor and outdoor environment monitoring applications by addition of the sensors as the interface is standardised.

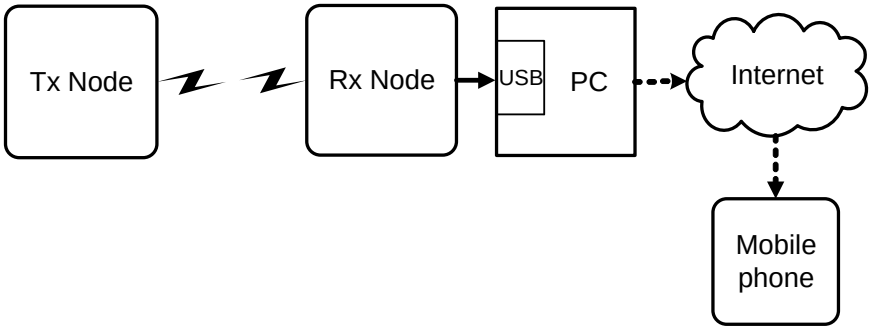

Figure 3.1: Proposed System Block Diagram

3.1.1 Wireless Sensor Node

Wireless sensor node is the main part of the any WSN based application. Wireless sensor node performs the tasks of sensing, processing and transmitting the necessary information to other wireless nodes. Designing of wireless sensor node includes interfacing of sensors, controlling or processing unit and radio modules.

The proposed modular wireless sensor node consists of a sensors array, switching logic, an ultra low power microcontroller and a wireless transceiver as shown in Fig. 3.2. Microcontroller has in built nanowatt extreme low power (XLP) technology. Switching logic is used to connect the particular sensor from the sensor array to the microcontroller. Internal structure of the switching logic is shown in Fig. 3.3. Each switching logic contains three switches with selection lines for each and one enable pin. Three selection lines of all switches are tied together for controlling all switches simultaneously. Selection line and enable line of the switching line is controlled by the microcontroller. Enable line of switching logic is used to

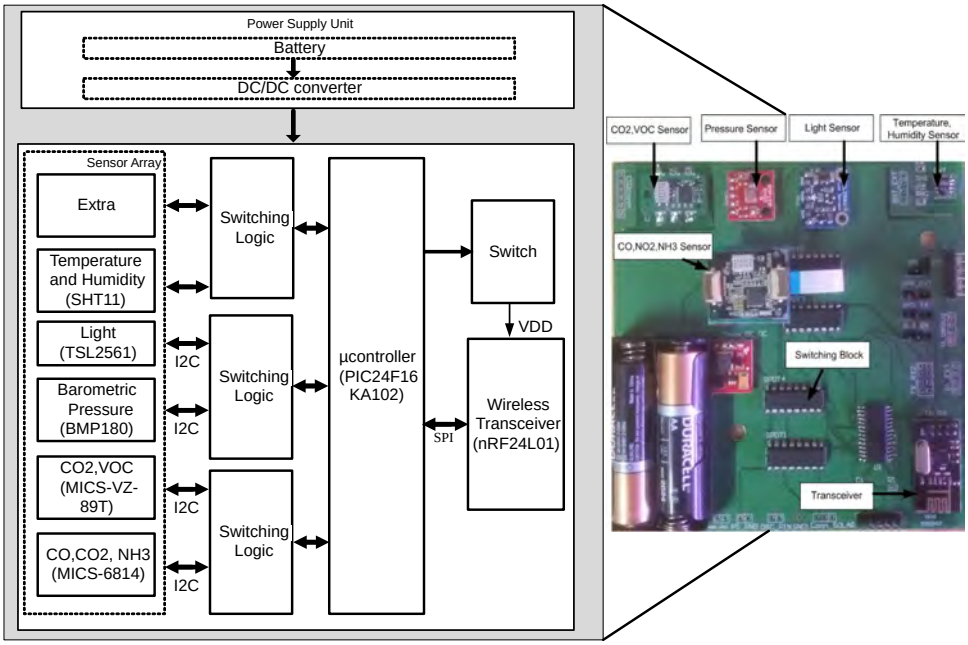

Figure 3.2: Proposed Wireless Sensor Node

enable particular switching logic and selection line selects the particular sensor. When selection line is zero supply will be available to the sensor-1 as well as SDA and SCL lines of the microcontroller will be connected to the SDA and SCL lines of the sensor-1. Logic one at the selection line selects the sensor-2 for interfacing to the microcontroller. Without switching logic block to interface n sensors (based on I2C interface) $3n$ pins of microcontroller are used. In proposed switching architecture for interfacing n sensors $(3n/2)$ +1 microcontroller pins are required for even value of n. For example for interfacing two sensors instead of 6 pins (3 pins for each; two for I2C interface and one for supply) only 4 pins of microcontroller are needed for interfacing, one for enable and one for selection and two for I2C interface. Proposed architecture saves $(3n/2)$-1 pins for interfacing, which helps in addition of more sensing parameters in future without adding processing unit. For interfacing n sensors $n/2$ switching logic blocks are needed.

Sensors data are processed by the μcontroller and transmitted through the wireless transceiver. Power supply of transceiver is given through switch

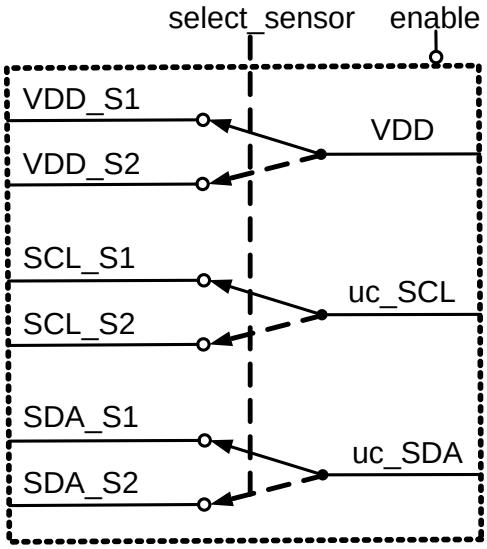

Figure 3.3: Switching Logic

for making it ON only for transmission. Which helps in power consumption reduction. Power is supplied to the wireless sensor node through DC/DC converter which is supplied by two AA batteries. The receiver node attached to a PC is powered by USB interface.

Table 3.1: Sensors Used in Wireless Sensor Node

Sensor	**Parameter**	**Range**	**Company**
SHT11	Temperature	-40 to 123.8 ° C	Sensirion
SHT11	Humidity	0 to 100 %RH	Sensirion
TSL2561	Light	0.1 to 30,000 lux	TAOS
BMP180	Barometric Pressure	300 to 1100 hPa	Bosch
MICS-6814	CO	1 to 1000 ppm	SGX
MICS-6814	NO_2	0.05 to 10 ppm	SGX
MICS-6814	NH_3	1 to 300 ppm	SGX
MICS-VZ-89T	CO_2	400 to 2000 ppm	SGX
MICS-VZ-89T	VOC	0 to 1000 ppb	SGX

3.1.1.1 Sensors

Detail about the sensors used in the wireless sensor node is given in Table 3.1. Selection of the sensors is based on the system requirement mentioned

earlier, such as long life span, accuracy of data, operating voltage and standardized interface. Implemented sensor node consists of SHT11 sensor [76] for measurement of temperature and humidity which provides fully calibrated digital output and can be treated as a golden standard. As a light sensor TSL2561 sensor [77] from TAOS is used which also provides calibrated digital output.

The BMP180 [78] is an ultra-low power, high precision digital barometric pressure and temperature sensor from Bosch Sensortec. It consists of a piezo-resistive sensor, an analog to digital converter, a control unit with EEPROM and a serial I2C interface. The calibration data is stored in EEPROM which is used to compensate offset, temperature dependence and other parameters of the sensor. The raw measurements of pressure and temperature are compensated for temperature effects and other parameters using the calibration data saved into the EEPROM. From the measured pressure, the altitude in meters can be calculated through international barometric formula. Sensor has ultra-low power consumption of 3 µA at one sample per second with operating voltage range of 1.8V to 3.6 V.

Gas sensors are classified into three categories based on the construction and working principle (i) Electrochemical (ii) Metal Oxide Semiconductor (MOS) and (iii) Optical. Each type of gas sensors has different characteristics and selection of a particular sensor depends on parameters like power consumption, cost, size, life time, sensitivity and response time. Electrochemical type of gas sensors have higher selectivity of particular gas and low power consumption but they have higher cost and shorter life span. Optical type of gas sensors have low energy consumption and longer life but they are expensive and bigger in size.

MOS sensors are used for the proposed work as MOS type of gas sensors are smaller in size, less costly, having fast response time and having longer life span compared to other sensors. MOS sensors consume more power compared to other sensors due to their operating principle, so trade off is observed between life span and power consumption. Construction of MOS sensor is shown in Fig. 3.4. For MOS sensors sensing layer is made up of

metal oxide generally SnO2. Oxygen is adsorbed on the surface of the sensing material. In the clean air condition, oxygen attracts the free electrons inside the metal oxide and forms the potential barrier for current flow at the grain boundary, which causes the restriction in current flow. When reducing gases comes in contact with sensing material it removes the few oxygen adsorbed on the surface of the sensing material, causes the reduction in resistance and increase in the current flow. Oxidizing gases add the oxygen species at the surface of the sensing material and causes the increase in the resistance. These reactions occur at higher temperature, which requires heater to heat the sensing layer. Thus with different concentration of the gases, variation in the resistance will be obtained.

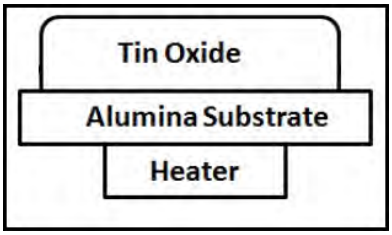

Figure 3.4: MOS Sensor Construction

The MOS gas sensor, MICS-VZ-89TD [79], from SGX Sensortech is used for measurement CO_2 and total VOC. Selected gas sensor can detect equivalent CO_2 and VOCs. It has low power consumption of 125 mW with operating voltage of 3.3V. It uses I2C interface and provides digital output for measured CO_2 and VOC.

The MOS gas sensor, MICS-6814 [80], from SGX Sensortech is used for measurement CO, NO_2 and NH_3. Selected gas sensor can detect CO, NO_2 and NH_3. The maximum limit of its power consumption is 150 mW with operating voltage of 3.3V. Selected sensor uses I2C interface for the communication. Variation of Rs/ Ro for the different concentration of the gas is provided in the datasheet of the sensor. Rs represent the sensing resistance and Ro represents the base resistance. Ro is the resistance obtained at the zero concentration of the target gas and Rs is measured for the different concentration of the gas. For deriving the gas concentration from the varying resistance of the sensor, data points are extracted from

the datasheet plots of Rs/ Ro versus gas concentration. From the extracted data points, plots are drawn again and based on power line curve fitting model and mathematical eqn. 3.1, eqn. 3.2 and eqn. 3.3 are derived. Derived equations are used for getting concentration of gases in ppm from the ratio of Rs and Ro.

$$CO(ppm) = 4.3104 * (Rs/Ro)^{-1.156} \tag{3.1}$$

$$NO_2(ppm) = 0.1587 * (Rs/Ro)^{0.998} \tag{3.2}$$

$$NH_3(ppm) = 0.6416 * (Rs/Ro)^{-1.851} \tag{3.3}$$

3.1.1.2 Microcontroller and Wireless Transceiver

Microcontroller works as controlling and processing unit in wireless sensor node. Microcontroller available in wide variety differs from each other in terms of architecture, number of bits, power consumption, operating frequency, instruction set, peripherals and interfaces available. Classification of the microcontroller is shown in Table 3.2. The microcontroller bus width can be either 8, 16 or 32 bit. The instruction set is either Complex Instruction Set Computer (CISC) or Reduced Instruction Set Computer (RISC). The memory architecture is either Harvard, modified Harvard or Von Neumann. The broadly used microcontrollers are 8051, Peripheral Interface Controller (PIC), AVR, Mixed Signal Microcontroller (MSP) and Advanced RISC Machine (ARM).

In wireless sensor node, microcontroller operates in different modes like active mode, idle mode, deepsleep mode. For all these modes current consumption plays important role in increasing life time of battery. Comparison between different type of microcontrollers is given in Table 3.3. PIC24F16KA102 controller based on extreme low power (XLP) technology form Microchip is used for reduction of power consumption.

In wireless sensor node, transceiver is highest power consuming block. The parameters like operating voltage, active current, idle current, operating

Table 3.2: Classification of Microcontrollers

Parameter	Type
Bus Width	8 bit
	16 bit
	32 bit
Memory Architecture	Harvard Architecture
	Von Neumann Architecture
	Modified Harvard Architecture
Instruction Set	Complex Instruction Set Computer (CISC)
	Reduced Instruction Set Computer (RISC)

Table 3.3: Specifications of Different Microcontrollers

Parameter	ATMEGA32L	MSP430G2553	PIC24F16KA102
Memory Architecture	Harvard	Von Neumann	Modified Harvard
Instruction Set	Advanced RISC	RISC	
Operating Voltage	2.7 V - 5.5 V	1.8 V - 3.6 V	1.8 V - 3.6 V
Flash Memory	32K	16K	16K
Active Current	1.1 mA at 1MHz, 3V	230 µA at 1 MHz, 2.2 V	down to 8 µA
Idle Current	0.35 mA at 1MHz, 3V	0.5 µA	down to 2 µA
Power down/Off Mode /Deep sleep current	<1µA	0.1 µA	down to 20 nA

frequency and range of operation play important role in the selection of transceiver. Comparison between different transceivers is shown in Table 3.4. An ultra low power transceiver nRF24L01 from Nordic [81] is used for wireless transmission and reception, which also supports to make low power wireless sensor node.

Table 3.4: Specifications of Different Transceivers

Manufacturer	Device	Frequency	Isleep[μA]	I TX 0dBm[mA]	Vdd
TI	CC2540	2.4 GHZ	1	21	2.0-3.7
Freescale	MC12311	300-900 MHz	1	25	1.8-3.6
SiLabs	Si4010	27-960 MHz	0.7	12	1.8-3.6
EM Marin	EM9201	2.4 GHz	0.8	14	1.9-3.6
Nordic	nRF24L01	2.4 GHz	0.9	11.3	1.9-3.6

3.1.2 Methodology for Sensing and Transmission

The operation of the wireless sensor node consists of two phases; (i) sensing and (ii) transmission. To quantify the energy consumption of transmitter node, its operation is divided into different states as shown in Table 3.5. States S1 to S7 represents the sensing phase of the wireless sensor node and

state S8 representing transmission phase. The bottom most row of the table shows the time duration of state for which particular module of wireless sensor node is active. For example, in state S2, the SHT11 and microcontroller are active for 0.31 *secs* and all other modules are inactive. This provides an intuitive representation to optimize the operation of the sensor node depending upon the power requirement of the application.

Table 3.5: Duration of Different States of the Wireless Sensor Node

Modules/States	**S1**	**S2**	**S3**	**S4**	**S5**	**S6**	**S7**	**S8**
μcontroller	deepsleep	active	active	active	active	active	S2 to S6 repeated twice	active
Transceiver	inactive	inactive	inactive	inactive	inactive	inactive		active
SHT11	inactive	active	inactive	inactive	inactive	inactive		inactive
TSL2561	inactive	inactive	active	inactive	inactive	inactive		inactive
BMP180	inactive	inactive	inactive	active	inactive	inactive		inactive
MICS-6814	inactive	inactive	inactive	inactive	active	inactive		inactive
MICS-VZ-89T	inactive	inactive	inactive	inactive	inactive	active		inactive
Time Duration	34 *secs*	0.31 *secs*	1.28 *secs*	1.88 *secs*	2.28 *secs*	0.2 *secs*		0.11 *secs*

Initially, switching on the power automatically puts the transmitter node in state S1, where it stays for 34 *secs*. In state S1 all modules are inactive. After that, it goes to state S2 during which time, SHT11 is setup and sensed data is written to the μcontroller memory. States S3 to S6 represents the active time for TSL2561, BMP180, MICS-6814 and MICS-VZ-89T sensors respectively. Duration of each state represents the time required for setup of sensor, sensing data and writing data into μcontroller memory. States S2 to S6 are repeated twice in state S7. In state S7, after the three sets of data are written to the μcontroller memory, a voting algorithm is performed to remove anomalies, if any. By doing so, the reliability of the data is enhanced and is shown in the results Section. Transceiver remains inactive for states S1 to S7 and after that in state S8 it becomes active and data is transmitted.

With the above sensing and transmission scheme, it is possible to quantify, in terms of power and time, the various states of the wireless sensor node at ease. This provides a scope for further optimization for future deployments. For example, if S1 is stretched during the sleep mode, the average power consumption is lowered, thereby prolonging the battery life. This is also explained and quantified in the experimental results.

Table 3.6 shows the power calculations for the sensor node. For different

Table 3.6: Power Calculation for the Sensor Node

Modules	**S1**	**S2**	**S3**	**S4**	**S5**	**S6**	**S8**
	Current (mA) for different states						
Microcontroller	6e-4	4.3	4.3	4.3	4.3	4.3	4.3
Transceiver	-	-	-	-	-	-	11.3
SHT11	-	1.26	-	-	-	-	-
TSL2561	-	-	1.15	-	-	-	-
BMP180	-	-	-	0.74	-	-	-
MICS-6814	-	-	-	-	43.4	-	-
MICS-VZ-89T	-	-	-	-	-	32	-
Total I (mA)	6e-4	5.56	5.45	5.04	47.7	36.3	15.6
Time (*secs*)	34	0.31	1.28	1.88	2.28	0.2	0.11
Multiplier of time	1	3	3	3	3	3	1
Total time (*secs*)	34	0.93	3.84	5.64	6.84	0.6	0.11
Voltage	3.3	3.3	3.3	3.3	3.3	3.3	3.3
Energy (mJ)	0.067	17.06	69.06	93.80	1076.68	71.87	5.66
Total Energy (mJ) =	1334.19						
Total Time (*secs*) =	51.96						
Average Power (mW) =	25.67						

states, total current is calculated by adding currents of all modules, according to their states as stated in Table 3.5. For each state, the final value of the time is obtained by multiplication of time and multiplier of time (repetition of time). For example, for state S2, final value of time is 0.93 *secs* which is obtained by multiplication of 0.31 *secs* and 3. Energy for different states is calculated by multiplication of total current, voltage and total time of particular state. Total energy is the summation of energy of all the states of the node. Total time calculated by summation of final value of time for all states is 51.96 *secs*. The average power of the sensor node is calculated by dividing the total energy by the total time period, and the result obtained is $25.67mW$.

3.1.3 IoT enabled Monitoring Platform

RX node is interfaced with PC through UART to USB converter. Received data is monitored in PC through GUI as shown in Fig. 3.5. GUI is developed to store and monitor data remotely for future analysis. It also transfers the monitored data through internet to smartphone. The monitored data will

be displayed in the numerical and graphical form for quick understanding and decision making. The interface between receiver node and GUI is plug and play type using USB port. The monitored data will be automatically stored through excel sheet with date and time information which is useful for further analysis.

GUI is developed in Laboratory Virtual Instrument Engineering Workbench known as LabVIEW. LabVIEW uses graphical programming language which allows acquisition, processing and controlling of data. LabVIEW program is known as Virtual Instrument (VI) because their appearance and operation imitate the actual instrument. VI consists of two components front panel and block diagram appears in the form of two separate windows. Front panel and block diagram both are linked to each other. Front panel represents different types of controls and indicators of VI while block diagram represents different functions and actual connection of the different components of VI.

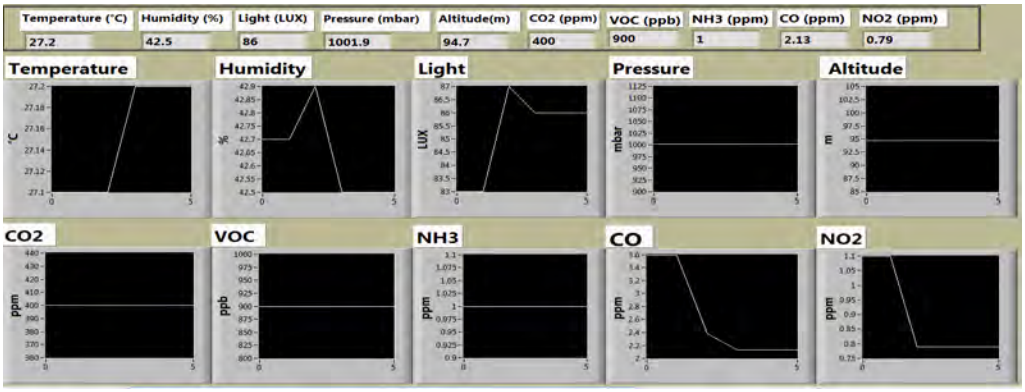

Figure 3.5: Graphical User Interface

Virtual Instrument Software Architecture (VISA) API is used to interface receiver node with LabVIEW. VISA software API provides interface between hardware and software development environment such as LabVIEW. VISA is also available in other languages. VISA is a standard I/O API for instrumentation programming. It is a standard for configuring, programming and troubleshooting instrumentation systems comprising GPIB, VXI, PXI, Serial, Ethernet, and/or USB interfaces. VISA uses the

same operations to communicate with any device, irrespective of interface and provides interface independence. VISA calls appropriate driver depending on the type of instrument connected so it is not required to learn instrument specific communication protocol. As VISA defines its own data types it prevents problem like size of an integer may be different for different platform. Application written in LabVIEW using VISA is easily portable from one platform to another. Thus VISA API greatly reduces development time as it is platform independent, bus independent, and environment independent. The same API can be used regardless of type of device, platform, or programming language.

In block diagram functions, VISA palette is available in Instrument I/O. Different VISA functions are available in it. In the developed VI VISA serial, VISA read and VISA close functions are used. VISA serial port function is used to configure the serial port for particular baud rate, data bits, parity, stop bits and flow control. VISA read function is used to read the data received. VISA close function is used to close the session so another application can access the port without exit from LabVIEW. Received data in addition to actual parameter values consists of character which is added to separate the parameter values. Match pattern and scan from string functions are used to separate the values of all different parameters. Separated values are displayed graphically and in the form of numeric on front panel of VI and enables simultaneous monitoring of all parameters.

Details about how connectivity is established for data from LabVIEW GUI to the Android based smartphone is discussed in our earlier work [75], [82], [83]. Fig. 3.6 shows the screenshot of the developed Android application. The developed Android application is tested on a smartphone based on Android 4.3.

3.1.4 Calibration

Calibration of sensors is one of the important factor for ensuring accurate results. Few reasons for the need of calibration are manufacturing

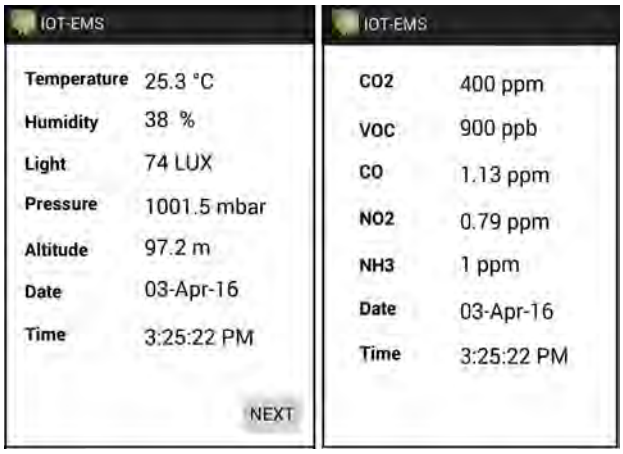

Figure 3.6: Android Application

variations even between two sensors, aging effect and effect of humidity, temperature, shock during storage, shipment and/or assembly may change sensor's response. There are different methods for the calibration from which curve fitting method is used for calibration. For the proposed wireless sensor node, calibration is done for temperature, humidity, light, CO and NO_2 parameters. Calibration model is derived using curve fitting tool in MATLAB by applying linear, polynominal and power models and selecting model having lowest RMSE.

Electronics add Quality Development Centre (EQDC) at Gandhinagar, Gujarat is providing facility for calibration of different instruments used in industries, academic institutes, administrative offices and service sector companies. Instruments available at EQDC are also calibrated by National Physical Laboratory (NPL) at the regular time intervals. Based on the availability of the instruments, calibration of temperature, humidity and light is done at EQDC and CO and NO_2 sensor calibration is done based on CPCB data.

Instruments used for the calibration of sensors at EQDC are mentioned in Table 3.7. Calibration model is required to be developed in the case of larger difference between sensor and reference instruments. After comparing the results of sensor and instruments, calibration model is derived if the large difference is found between sensor and reference readings. There are different

Table 3.7: Instruments Used for Calibration

Sensor	Instruments	Company
SHT11	Climate Chamber (C340)	Weiss
BMP180	Pressure Calibrator (717)	Fluke
TSL2561	Digital illuminance meter (51002)	Yokogawa

methods for deriving calibration model from which curve fitting method is used.

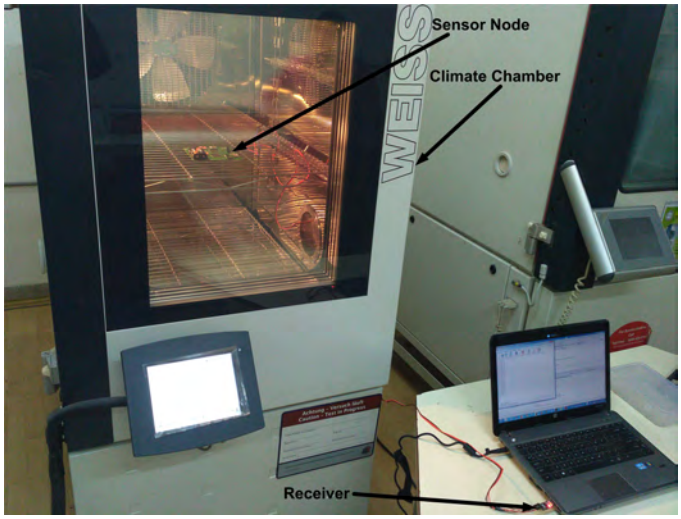

Figure 3.7: Setup for Calibration of Temperature/Humidity Sensor

Setup for the calibration of SHT11 sensor for temperature and humidity is shown in Fig. 3.7. Sensor node was kept in chamber and data is logged in the computer through UART interface. During the calibration process for temperature, chamber temperature is set for different temperatures and readings of the sensor and chamber are taken. Chamber readings are taken as reference readings. Considering the normal range of temperature, readings are taken from 20°C to 50°C. Readings are taken for four different temperatures 20° C, 30°C, 40°C and 50°C. For each temperature, five readings are taken and compared with the readings of chamber. Difference values between sensor readings and reference readings are in the range of accuracy specified by the manufacturer, so no calibration model is needed. Fig. 3.8 shows the plot for the sensor and reference readings which are close

Table 3.8: Calibration Models for Humidity and Light Sensors

Parameters	**Model**	**Equation**	**RMSE**
Humidity	power	0.1323*sensor $^{1.428}$	0.499
Light	polynominal	0.7217*sensor + 52.24	75.538

to each other.

For calibration of relative humidity, considering normal range of humidity, readings are taken from 30% RH to 80%RH at 25°C. Readings are taken for four different RH 30% RH, 45% RH, 60% RH and 80% RH. For each RH value, five readings are taken and compared with readings of chamber. As higher difference is found between reference and sensor readings, than mentioned by manufacture, calibration model is developed for the same as per Table 3.8. Fig. 3.9 shows the plot for comparison of reference data with sensor data and calibrated data. Reference data and calibrated sensor readings are close to each other.

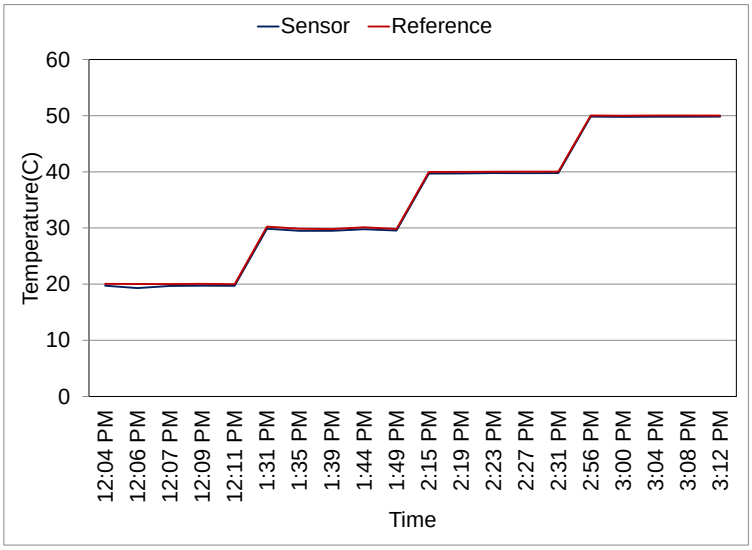

Figure 3.8: Sensor and Reference Data for Temperature

Setup for the calibration of TSL2561 sensor is shown in Fig. 3.10.

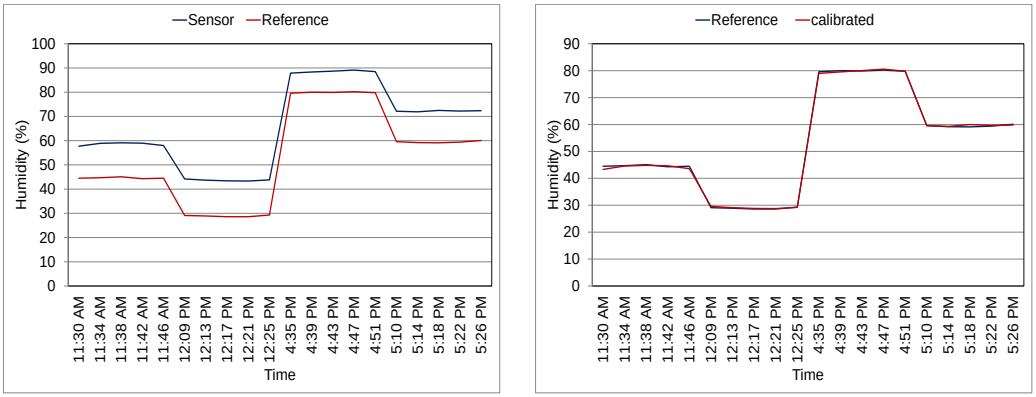

(a) Sensor and Reference Data (b) Sensor and Calibrated Data

Figure 3.9: Humidity

Figure 3.10: Setup for Calibration of Light Sensor

Sensor node was kept in different light intensity environments. In different light intensity environments, readings are taken. Higher difference between sensor and reference readings are found for higher range of light intensity so calibration model is developed for the same as per Table 3.8. Fig. 3.11 shows the plot for comparison of reference data with sensor data and calibrated data. Reference data and calibrated sensor readings are close to

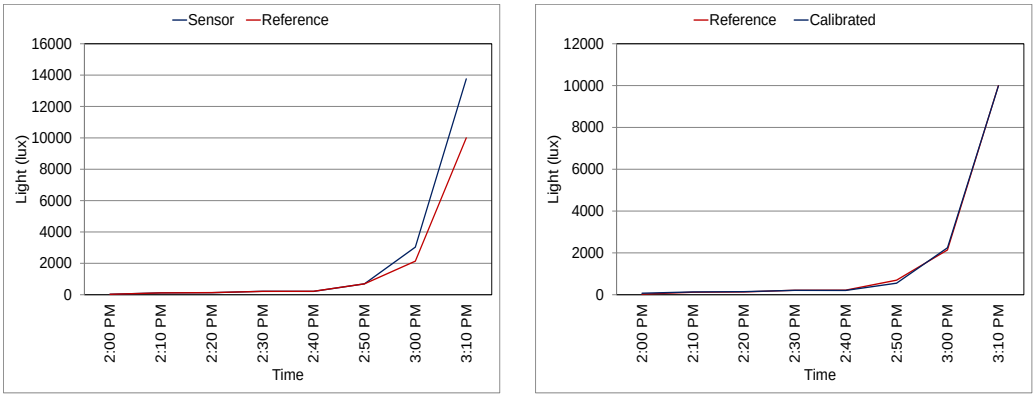

(a) Sensor and Reference Data (b) Sensor and Calibrated Data

Figure 3.11: Light

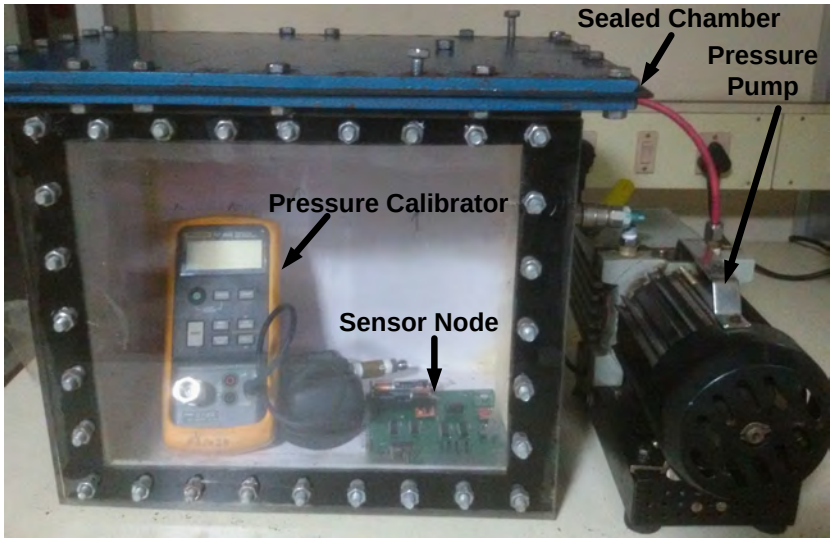

Figure 3.12: Setup for Calibration of Pressure Sensor

each other.

Setup for the calibration of BMP180 sensor is shown in Fig. 3.12. Sensor node was kept in small sealed chamber and receiver was connected to computer. Data is logged in the computer through RX via UART interface. During the calibration, process pressure is set for different pressure values and readings of the sensor and chamber are taken.

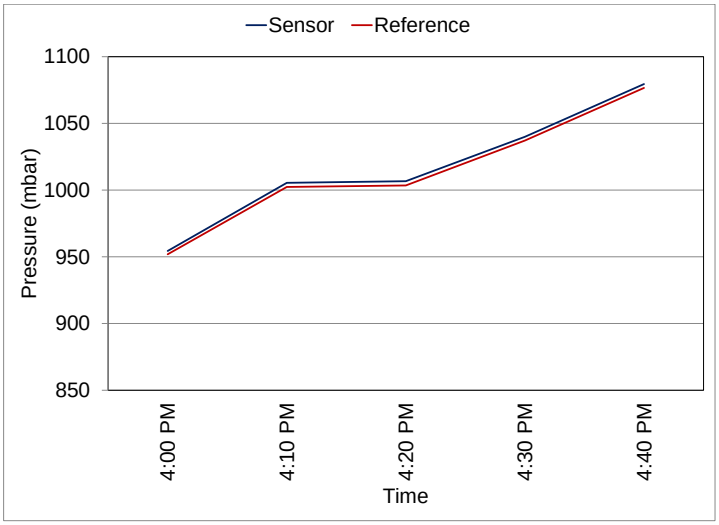

Figure 3.13: Sensor and Reference Data for Barometric Pressure

Considering the normal range of barometric pressure, readings are taken from 900 mbar to 1100 mbar. Readings are taken for six different pressures. Difference values between sensor readings and reference readings are in the range of accuracy specified by the manufacturer, so no calibration model is needed. Fig. 3.13 shows the plot for the sensor and reference readings which are close to each other.

Monitored data by CPCB instruments at Maninagar station, Gujarat were considered as reference data for calibration of CO and NO_2 sensor. Table 3.9 shows the instruments used at CPCB, Maninagar station. For calibration wireless sensor node was deployed at CPCB, Maninagar station for three days in different time slots. Readings were taken at the interval of 10 *secs*.

From the sensed values of CO and NO_2, Rs extracted from eqn. 3.1, eqn. 3.2 and eqn. 3.3. For CO and NO_2 sensor, Rs value is affected by temperature and humidity. Equations presented in Table 3.10 are used for considering temperate and humidity effect on CO and NO_2 reading for ensuring accuracy. Where Rs_RH is the sensing resistance at the measured

Table 3.9: Instruments Used for Monitoring Parameters at Maninagar Station, CPCB

Parameters	Instruments	Company
CO	Carbon monoxide analyser (CO12M)	Environment S.A
NO2	Nitrogen oxides analyzer (AC32M)	Environment S.A

humidity, RH is measured humidity, Rs_T is the sensing resistance at the measured temperature and T is the measured temperature.

Table 3.10: Temperature and Humidity Dependence of CO and NO_2

Sensing parameter	Environment parameter	Equation
CO	Temperature	$Rs(25°C) = Rs\_T * (0.038 * (T-25) + 1.013)$
CO	Humidity	$Rs(50\%RH) = Rs\_RH * (-1.6 * 10^{-5} * (RH-50)^2 - 6.5 * 10^{-4} * (RH-50) + 1$
NO_2	Temperature	$Rs(25°C) = Rs\_T * (3 * 10^{-3} * (T-25)^2 + 2.7 * 10^{-2} * (T-25) + 1)$
NO_2	Humidity	$Rs(50\%RH) = Rs\_RH * (2.4 * 10^{-5} * (RH-50)^2 + 1.9 * 10^{-3} * (RH-50) + 1)$

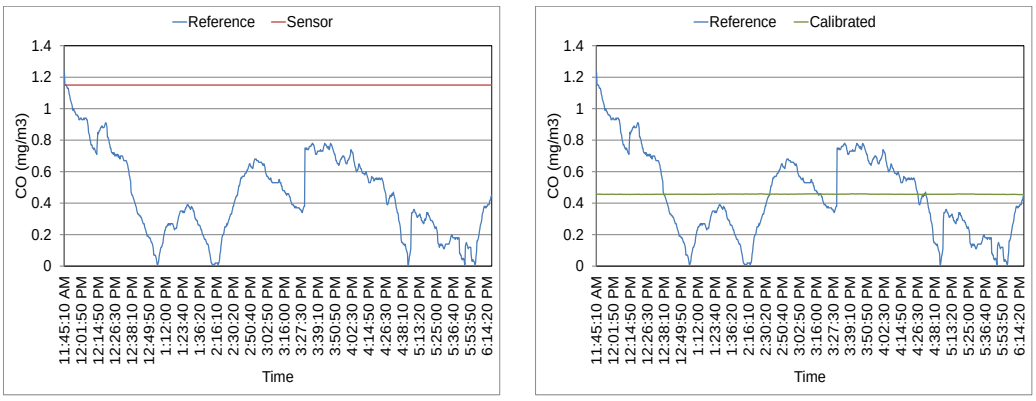

(a) Reference and Sensor Data (b) Reference and Calibrated data

Figure 3.14: Carbon Monoxide (CO)

Calibrated values of temperature and humidity are used in the equations of Table 3.10. Rs/Ro ratio for CO and NO_2 is converted back into ppm concentration through eqn. 3.1, eqn. 3.2 and eqn. 3.3. In Fig. 3.14 and Fig. 3.15 for each parameter reference data is compared with sensor data and calibrated data. Sensors measure value in ppm, it is converted into mg/m^3

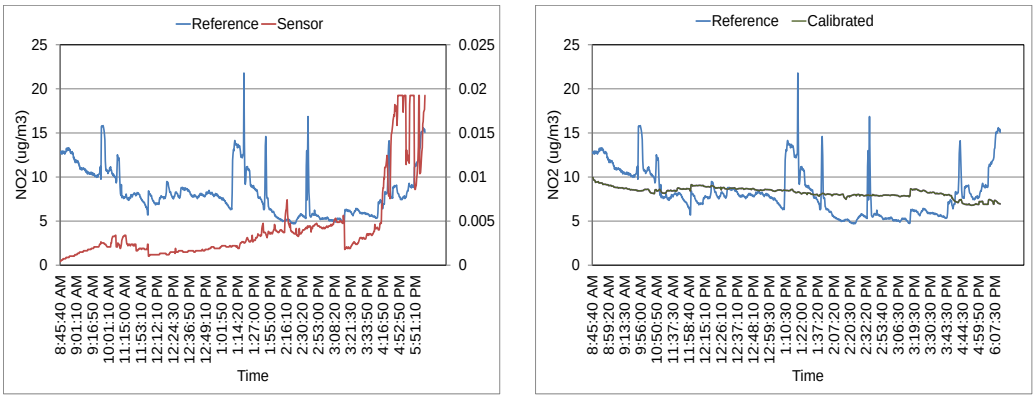

(a) Reference and Sensor Data (b) Reference and Calibrated Data

Figure 3.15: Nitrogen Dioxide (NO_2)

and µg/m^3 for CO and NO_2 respectively for comparison with CPCB data. Some spikes observed in the reference data can be considered as anomalies. This can be removed through smoothing or averaging techniques. After the calibration, reference data matches with calibrated data and RMSE for each parameter is quiet less and acceptable. For CO very less variations in the reading compared to reference data, reason is after applying eqn. 3.1, CO value is restricted to a particular lower limit. For getting lower value readings this restriction can be removed through programming. Table 3.11 shows the details about the applied models for calibration and RMSE obtained for each parameter.

Table 3.11: Calibration Models for CO and NO_2

Parameters	**Model**	**Equation**	**RMSE**
CO	power	$0.4485*CO\_sensor^{-0.05995}$	0.266
NO2	power	$4.976*NO_2\_sensor^{-0.09707}$	2.587

The variance indicates how far each value in the data set is from the mean. For CO data Table 3.12 shows variance of reference data, sensor data and calibrated data are not far away from mean value. To handle aging or shock effects it is required to do periodic calibration using standard

instruments. Based on the calibration it is required to reduce the difference between standard value and actual value. For which calibration model can be derived using curve fitting method. Then derived calibration model in terms of equations can be incorporated into the system through modification in application software.

Table 3.12: Variance

Parameter	**Variance**
Reference Data	0.001933
Sensor Data	0.002978
Calibrated Data	0.000467

3.2 Experimental Results and Deployment

Deployment of the proposed system in the laboratory is done by placing the sensor node and receiver node at a distance of 6 meters from each other. Sensor node and receiver node are kept in different rooms which are separated by walls. With this deployment, reliability of the data transmission is checked for transmission of 1000 samples from TX node to RX node. As shown in Table 3.13, reliability obtained is 97.4% as from 1000 data at RX node 974 data are received correctly.

Time between two measurements is equal to the summation of sleep time, sensing time and transmitting, considered as measurement cycle. For the measurement cycle of 51.96 *secs*, power consumption of the sensor node is $25.67mW$ as shown in Table 3.6. The rating of two AA Duracell used is 2850 mAh and provides 3V output. Sensor node life time can be calculated by dividing input energy by power consumption. For the measurement cycle of 51.96 *secs*, lifetime of battery is equal to 13.87 days. Varying measurement cycle will change the lifetime of the battery. As sensing and transmission time is fixed, prolonging the duration of S1 state (sleep time), lifetime of the battery can be increased. Table 3.14 shows the lifetime of battery for different measurement cycle with varying sleep time. Depending on the application requirement particular measurement cycle can be selected. Removing voting

algorithm and taking only one reading for each parameter per measurement cycle will also increase the lifetime of battery but at the cost of reliability.

Table 3.13: Reliability of Data Transmission

Expected Number of packets	**Number of correctly received packets**	**Reliability(%)**
1000	974	97.4

Table 3.14: Battery Life Time

Measurement cycle (min)	**No of Days**	**No of Months**
1	16	-
2	32	1
10	160	5
30	479	16
60	956	31.8

3.3 Conclusion

We have presented IoT enabled wireless environment monitoring system to monitor ten different parameters related to environment in this Chapter. For the proposed system we tried to achieve the low power consumption, high reliability of transmission, accuracy of data and remote monitoring. Proposed system is calibrated against standard instruments to improve the accuracy of the results. Using proposed hardware of sensor node $(3n/2)$ -1 pins are saved for interfacing where n is even number of sensors. Achieved reliability of transmission for the developed system is 97.4%. Power consumption of the sensor node is $25.67mW$ and can be lowered by increasing the sampling time of the node. Battery life achieved for the sensor node is approximately 31 months for the measurement cycle of 60 *secs*. IoT enabled monitoring platform is used for remote monitoring and storage of real time data. The proposed system is validated through deployment inside and outside the laboratory. Deployment results of the proposed system for different applications are discussed in Chapter 5.

As discussed in Chapter 2, prediction model for PM2.5 can be developed based on the correlation of PM2.5 with precursor gases. IoT enabled wireless sensor node discussed in this Chapter will be useful in finding the concentration of precursor gases. Prediction model can be implemented in sensor node for getting value of PM2.5 based on precursor gases. Implementation of PM2.5 prediction model helps in monitoring PM2.5 without the need of power hungry gas sensors and big sized, costly analyzers. Development and implementation of prediction model for PM2.5 are discussed in Chapter 4.

Chapter 4

Prediction Model for PM2.5

It is possible to find the concentration of PM2.5 from the concentration of the precursor gases [3]. Prediction of PM2.5 from the concentration of correlated precursor gases eliminates the need of costly and bulkier instruments as well as power hungry sensors. In Chapter 3 we have discussed the development and deployment results of the IoT enabled wireless sensor node which can be used for finding the concentration of precursor gases. This Chapter focuses on the development of analytical equations based prediction model for PM2.5. In this work, we have selected PM2.5 as a target parameter because as discussed in Chapter 2, it is considered as one of the important parameters for finding AQI.

Developing prediction model is a part of supervised machine learning, which needs large dataset for the training. In Section 4.1 results related to correlation of precursor gases with PM2.5 is discussed. Based on the correlation study, developed prediction model in terms of simple analytical equations is discussed. Results related to testing of prediction model are provided in Section 4.2 followed by conclusion in Section 4.3

ANN is one of the technique which has been used for the forecasting wide range of pollutants and their concentration with very good results [28, 33, 36]. Previous research work study also shows performance of ANN is generally superior in comparison to traditional statistical methods, such as multiple linear regression, regression trees and autoregressive models [29, 30, 34, 84–86].

4.1 Model

Developing prediction model is equivalent to finding the output variable which is the good estimate of the target value using the known inputs set. Mostly for environment monitoring number of parameters affecting the target and relationship between inputs and output is not linear. Different techniques are available for the prediction from which ANN is selected based on the comparison given in earlier research work for different prediction models.

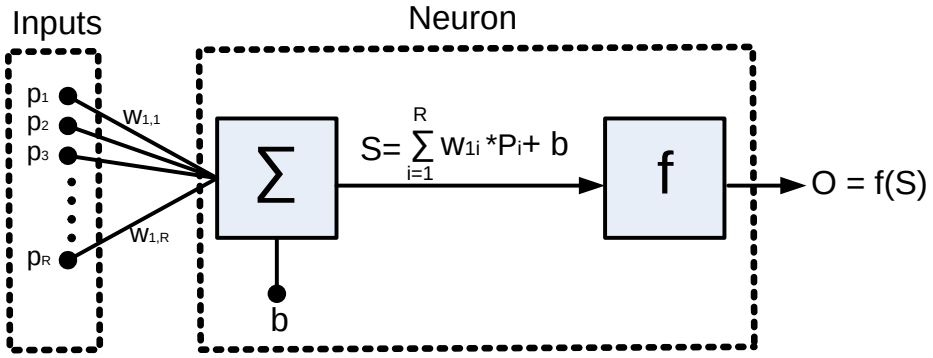

Figure 4.1: ANN's Neuron Model

ANN is inspired by biological nervous system. ANN consists of interconnected computing elements (neurons) each having inputs and outputs. As shown in Fig. 4.1, the model has R inputs each with different weight W. The sum (S) of weighted inputs and bias (b) is fed to the transfer function block (f). The output of each neuron is obtained by the sum of weighted inputs and bias and then applying the transfer function. Conventionally three types of transfer functions in tan-sigmoid, log-sigmoid and linear are used based on the application requirement and the output range [87].

In the proposed work ANN is used for nonlinear regression which is useful for prediction of output parameter in nonlinear combination of the one or more input parameters. For developing PM2.5 prediction model feed forward neural network is used which is made up different layers. These layers are arranged like a chain structure with each layer being a function of the layer

that preceded it. Each layer can be represented in the form of activation function, weights and biases.

Our proposed prediction model is derived using the following standard steps.

1. Collection of large sets of Input Data
2. Preprocessing of the Input Data
3. Selection of Topology
4. Number of iterations for training and validating the network
5. Number of iterations for testing the network
6. Network selection based on performance indices
7. Output is predicted based on the Predictors

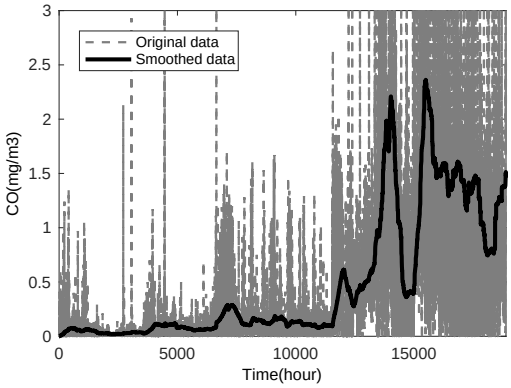

Figure 4.2: CO Data

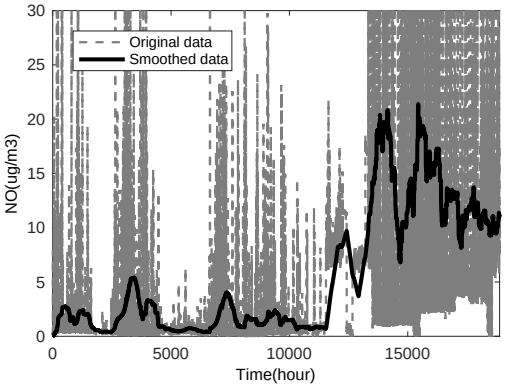

Figure 4.3: NO Data

To select the inputs for the prediction model it is necessary to obtain the correlation and cross correlation of the pollutants. In the proposed study, 41 months of hourly data [Step I] taken related to CO, NO, NO_2, SO_2, O_3, temperature, humidity, VOC (Benzene, Toluene, Ethyl Benzene, M+P Xylene, O-Xylene) and PM2.5 from a CPCB online station, India (N 23° 0' 16.6287, E 72° 35' 48.7816). Data obtained from CPCB online

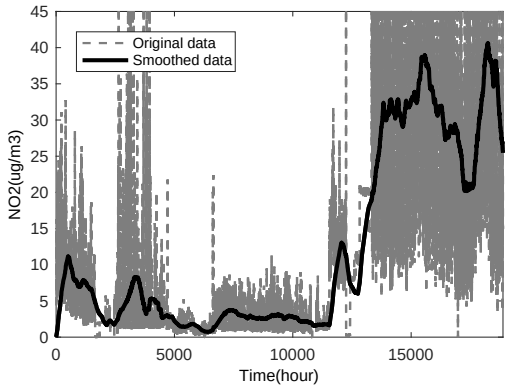

Figure 4.4: NO_2 Data

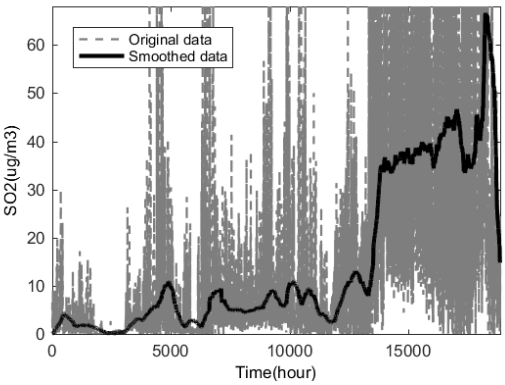

Figure 4.5: SO_2 Data

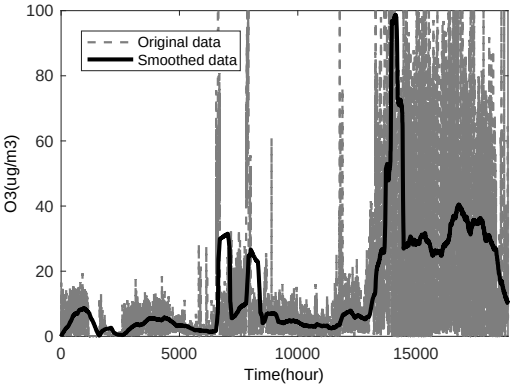

Figure 4.6: O_3 Data

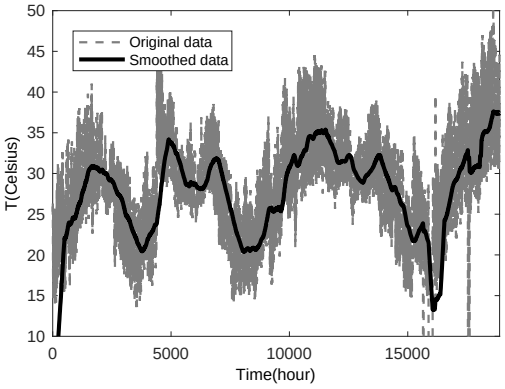

Figure 4.7: Temperature Data

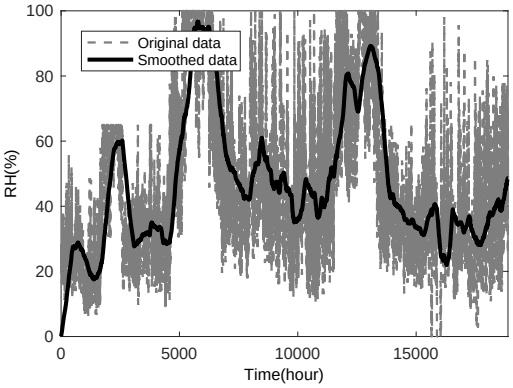

Figure 4.8: Humidity Data

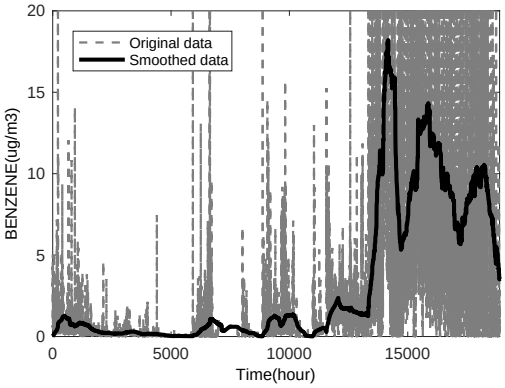

Figure 4.9: Benzene Data

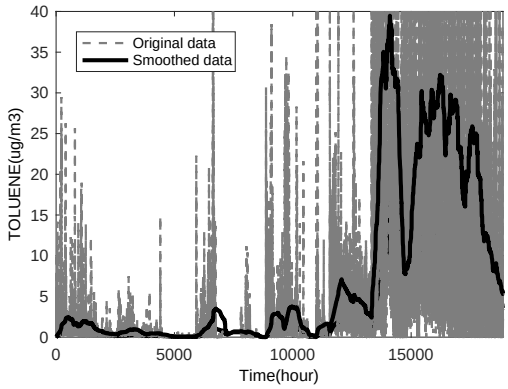

Figure 4.10: Toluene Data

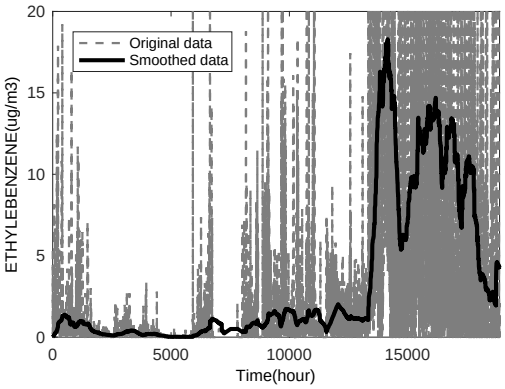

Figure 4.11: Ethyl Benzene Data

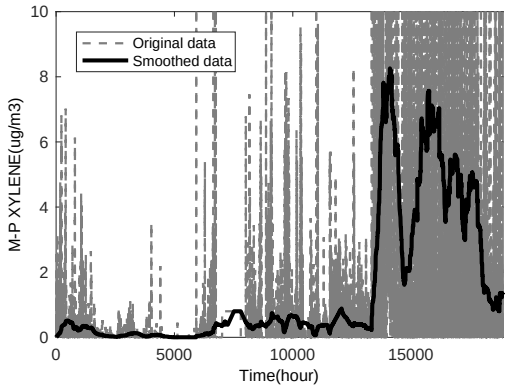

Figure 4.12: M-P Xylene Data

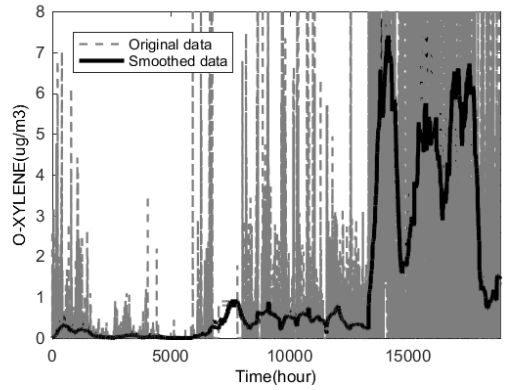

Figure 4.13: O-Xylene Data

station for all parameters was containing a total of 29,928 data. Due to maintenance, all the parameters data were not available simultaneously for 29,928 data. After removing maintenance data for each of the parameters, 18,880 data were available simultaneously for all parameters. These 18,880 data were smoothed out to remove the outliers [Step II] and is treated as the golden standard. Smoothing of the data is done through moving average filter, which was implemented in MATLAB. Window size used for smoothing was 500, which was selected, considering optimum size of window for which reasonably smoothed data was obtained. After smoothing, the first 500 data were removed, as the window size taken for averaging was for 500 data. So, smoothed data of 18,380 was used for

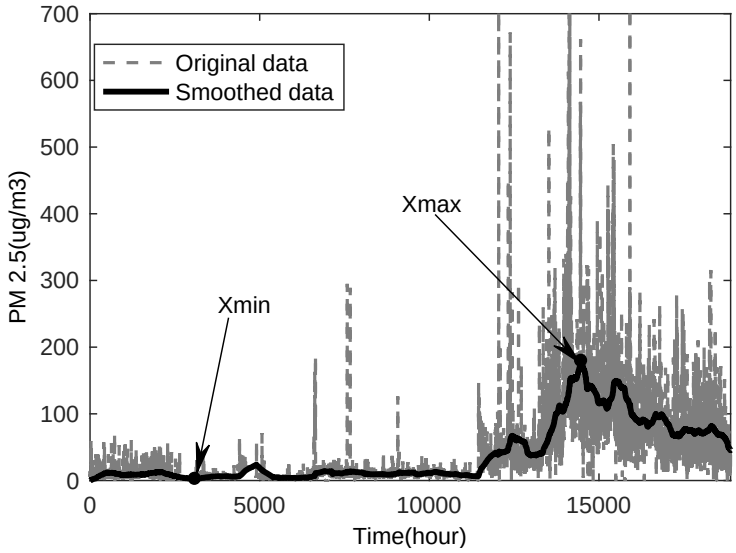

Figure 4.14: PM2.5 Data

developing prediction model. Fig. 4.2 to Fig. 4.14 shows the original and smoothed data for different pollutants.

Correlation between two parameters x and y can be represented by eqn. 4.1. Where R is correlation coefficient, x represents the first parameter data, y is the second parameter data and n is the total number of values. The value of R remains between −1 to +1. The +and −signs are used for positive correlation and negative correlation respectively. If x and y have a strong positive correlation, value of R will be close to +1. If x and y have a strong negative correlation, value of R will be close to −1. For practical purpose, correlation greater than 0.8 is assumed being strong and less than 0.5 as weak [88].

$$R = \frac{n(\sum xy) - (\sum x)(\sum y)}{\sqrt{(n\sum x^2 - (\sum x)^2) * (n\sum y^2 - (\sum y)^2)}} \tag{4.1}$$

Correlation and cross correlation, of the particulate matter PM2.5 with other gases and among the gases are evaluated based on the 18k+ data over the 41 months and as shown in Table 4.1. As can be seen, the highest correlation of PM2.5 is found with NO, NO_2 and Benzene and low

Table 4.1: Cross Correlation of Different Parameters

	CO	**NO**	**NO_2**	**SO_2**	**O3**	**T**	**RH**	**Ben**	**Tol**	**Eth**	**M-xyl**	**O-xyl**	**PM2.5**
CO	1	0.936	0.872	0.828	0.771	-0.069	-0.215	0.901	0.928	0.908	0.921	0.894	0.830
NO	0.936	1	0.927	0.826	0.789	-0.122	-0.230	0.927	0.927	0.909	0.907	0.860	0.909
NO_2	0.872	0.927	1	0.927	0.728	-0.075	-0.313	0.919	0.849	0.828	0.809	0.769	0.909
SO_2	0.828	0.826	0.927	1	0.714	0.009	-0.328	0.881	0.817	0.790	0.766	0.769	0.845
O_3	0.771	0.789	0.728	0.714	1	-0.066	-0.238	0.844	0.849	0.849	0.833	0.833	0.773
T	-0.069	-0.122	-0.075	0.009	-0.066	1	0.294	-0.126	-0.158	-0.191	-0.217	-0.127	-0.080
RH	-0.215	-0.230	-0.313	-0.328	-0.238	0.294	1	-0.318	-0.297	-0.323	-0.315	-0.324	-0.222
Benzene	0.901	0.927	0.919	0.881	0.844	-0.126	-0.318	1	0.956	0.943	0.934	0.891	0.919
Toluene	0.928	0.927	0.849	0.817	0.849	-0.158	-0.297	0.956	1	0.989	0.982	0.955	0.877
Ethyl benzene	0.908	0.909	0.828	0.790	0.849	-0.191	-0.323	0.943	0.989	1	0.989	0.963	0.880
M-P Xylene	0.921	0.907	0.809	0.766	0.833	-0.217	-0.315	0.934	0.982	0.989	1	0.964	0.855
O-Xylene	0.894	0.860	0.769	0.769	0.833	-0.127	-0.324	0.891	0.955	0.963	0.964	1	0.818
PM2.5	0.830	0.909	0.909	0.845	0.773	-0.080	-0.222	0.919	0.877	0.880	0.855	0.818	1

correlation with temperature and humidity. A strong correlation of CO, NO_2, SO_2 and VOC (Benzene, Toluene, Ethyl Benzene, M+P Xylene, O-Xylene) with PM2.5 is observed that is useful in selecting the inputs for the PM2.5 prediction model.

The proposed prediction model is based on supervised learning, where both inputs in pollutants: CO, NO_2, SO_2 and VOC (Benzene, Toluene, Ethyl Benzene, M+P Xylene, O-Xylene) and target (PM2.5) values are provided as a training data set. It is observed that the training of the network is efficient if each parameter of the training data set is normalized within the range [-1,1]. Normalization of the parameters is done by finding the value of each parameter within the minimum and maximum value using eqn. 4.2.

$$x_n = \frac{(Ymax - Ymin) * (X - Xmin)}{(Xmax - Xmin)} + Ymin \tag{4.2}$$

Where X is value of the parameter and $Xmax$ is the maximum value of the parameter and $Xmin$ is the minimum value of the parameter. For example, in CO data, X is the smoothed value of CO while $Xmax$ and $Xmin$ are maximum and minimum values of smoothed CO data respectively. As normalization range is within [-1,1], $Ymax$ is 1 and $Ymin$ is -1. The normalized parameters can be converted back into their original form using eqn. 4.3.

$$X = \frac{(x_n - Ymin) * (Xmax - Xmin)}{(Ymax - Ymin)} + Xmin \tag{4.3}$$

Where x_n represents normalized data and X is the smoothed data. $Xmax$ and $Xmin$ are the maximum and minimum values of smoothed data

respectively. For example, to convert the normalized data of predictand PM2.5 into original form, $Xmax$ and $Xmin$ values of targeted PM2.5, shown in Fig. 4.14 are used.

The total available data of 18k+ is divided into two sets first set includes 90% of data and second set includes 10% of data. The division into two sets is done randomly so that all types of data can be included in two sets. The 10% data is kept as unseen data for testing and comparing the performance of trained neural networks. Remaining 90% data is used for designing the neural network and it is divided as per artificial intelligence community which is 70% for training, 15% for validating and 15% for testing. The prediction model of PM2.5 shown in Fig. 4.15 is based on a feed forward neural network with single hidden layer [Step III]. The eight pollutants are the input parameters for each neuron of the hidden layer.

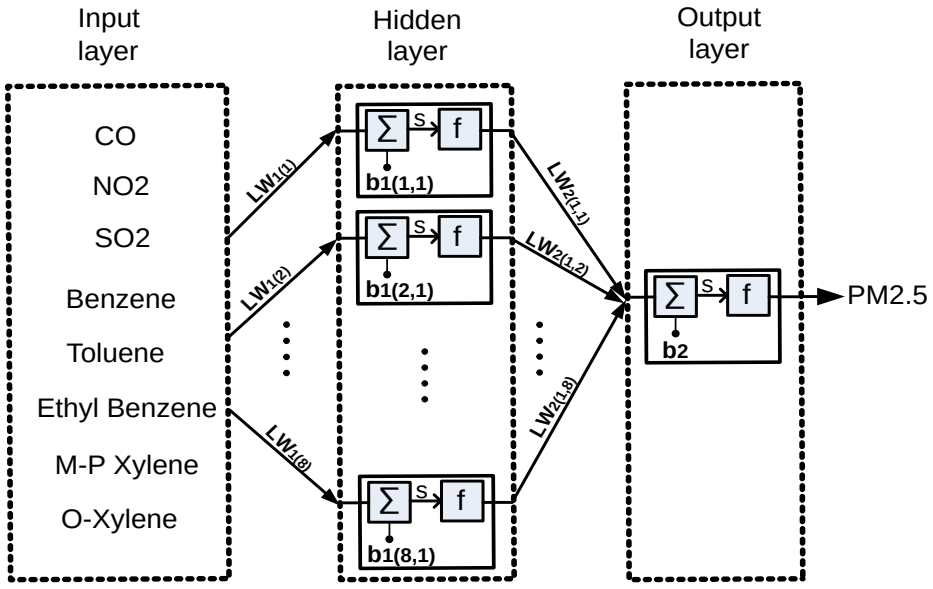

Figure 4.15: Selected ANN Topology for Prediction

In the model, the weights of hidden layer and output layer can be represented by matrix of the size S×R, where S is equal to the number of neurons in the layer and R is equal to the number of inputs of the layer. So, the matrix size of the hidden layer weights is 8×8 as the number of inputs and number of hidden layer size both are 8. The output layer weights

matrix size is 1×8 as output layer consists of one neuron and eight inputs coming from the hidden layer. For predicted model, weights of the hidden layer and output layer is represented by LW_1 of size 8×8 and LW_2 of size 1×8 respectively. $LW_{1(1)}$ represents the first row of LW_1 matrix, which is formed by the weights of inputs going to first neuron of the hidden layer. $LW_{2(1,1)}$ represents the first row and first column element of matrix LW_2. Biases of the particular layer can be represented by matrix of the size S×1, where S is equal to the number of neurons in the layer. b_1 and b_2 are bias matrices for hidden layer and output layer respectively. As the number of neurons in the hidden layer and output layer is 8 and 1 respectively, b_1 is 8×1 and b_2 is 1×1. $b_{1(1,1)}$ represents the first row and first column element of matrix b_1.

A standard *trainlm* function is used for training which is based on Levenberg-Marquardt algorithm [89, 90]. As the output range is positive, *logsig* transfer function is used for the hidden layer and *purelin* transfer function is used for the output layer. The *logsig* transfer function is represented by eqn. 4.4, where n is the input given to the transfer function. In *logsig* transfer function, output will be in the range of [0-1] for positive to negative range of input. In *purelin*, transfer function output is equal to the input.

$$logsig(n) = \frac{1}{(1 + e^{-n})} \tag{4.4}$$

Algorithm 1 Pseudo Code for Multiple Training of ANN

```
load the training set and testing set of data
for i = 1 to 100 do
    Train the network
    Evaluate training performance
    Evaluate testing performance
    Save network weights and biases
    Save trained network
end for
```

The pseudo code for multiple neural network training is shown in Algorithm 1. This algorithm is repeated 100 times to get the performance

of 100 different ANNs for comparing training and testing results with good generalization [Step IV, V]. For all 100 iterations, the training set is kept the same for all ANNs. After the training, the testing is done again for all 100 ANNs keeping the same testing data set for all ANNs to evaluate the performance.

Performance of the network is evaluated based on two standard parameters; RMSE and R^2. RMSE represents the square root of the average of the square of all errors, i.e. the difference between actual value or target and the predicted value [Step VI]. RMSE is represented by eqn. 4.5. Where, A_i represents the actual value, P_i represents the predicted value and n is the number of values.

$$RMSE = \sqrt{\frac{\sum_{i=1}^{n}(A_i - P_i)^2}{n}} \tag{4.5}$$

R^2 is also known as coefficient of determination which is represented as square of R, shown in eqn. 4.1. R^2 is used for multiple regression when prediction of a variable is based on the value of two or more variables. R^2 represents the relationship between the targets and network outputs. R^2 indicates how close the predicted outputs are to the targets. Range of R^2 is between 0 to 1. Value of R^2 nearer to 1 represents targets and predicted network outputs that are close to each other.

Initially, the model had a larger number of inputs than selected and not discussed here. This was primary because with large number of inputs complexity was more with comparable RMSE. The computation cost of an ANN model can be reduced by reducing the number of inputs, so the following model with less number of inputs is selected.

In prediction model number of inputs are reduced based on correlation results. Results of Table 4.1 show higher correlation of CO, NO_2, SO_2 and VOC (Benzene, Toluene, Ethyl Benzene, M+P Xylene, O-Xylene) with PM2.5 which stay above 0.8. This offers an opportunity to develop a prediction model based on CO, NO_2, SO_2 and VOC without considering other parameters. In prediction model, the number of input parameters is optimized from 12 to 8, which are CO, NO_2, SO_2 and VOC parameters

(Benzene, Toluene, Ethyl Benzene, M+P Xylene, O-Xylene).

4.1.1 Model Equations

The model consist of weights of the hidden layer and output layer that are shown by eqn. 4.6 and eqn. 4.7 respectively. The biases of the model for hidden layer and output layer are given by eqn. 4.8 and eqn. 4.9 respectively. Matrix B_1 is formed by repeating the hidden layer bias matrix b_1, N times, where N is equal to the number of testing data (1838 in our case). This operation shown by eqn. 4.10, is performed to make bias matrix size B_1 equal to the size of product term matrix $LW_1 * x_n$, so that addition operation $(B_1 + LW_1 * x_n)$, shown in eqn. 4.11 can be performed.

$$LW_1 = \begin{bmatrix} -25.978 & -31.063 & 17.505 & 38.446 & -37.353 & 97.708 & -92.951 & 65.964 \\ 3.295 & 6.460 & 0.203 & -1.981 & 10.078 & -10.281 & 3.352 & -3.782 \\ -2.661 & 2.503 & -1.075 & -1.011 & -0.194 & 1.702 & -2.768 & 1.690 \\ -6.069 & 6.142 & -2.212 & -3.593 & 1.800 & -3.002 & 0.222 & 2.803 \\ -9.788 & -7.748 & -4.424 & 27.227 & -4.406 & 0.016 & -6.279 & 8.460 \\ 3.821 & -6.233 & 1.243 & -1.449 & 5.600 & 1.846 & 1.801 & -5.862 \\ 3.149 & 6.319 & 0.368 & -0.825 & 10.746 & -11.220 & 2.650 & -3.428 \\ -2.127 & 1.991 & -1.116 & -0.032 & 0.038 & 4.094 & -4.882 & 1.330 \end{bmatrix} \tag{4.6}$$

$$LW_2 = [\,0.158 \;\; -17.591 \;\; -6.481 \;\; 1.614 \;\; -0.369 \;\; -0.817 \;\; 17.345 \;\; 4.950\,] \tag{4.7}$$

$$b_1 = \begin{bmatrix} 34.474 \\ 4.001 \\ -1.015 \\ -2.615 \\ 5.700 \\ -0.148 \\ 4.383 \\ -1.959 \end{bmatrix} \tag{4.8}$$

$$b_2 = [\,1.593\,] \tag{4.9}$$

$$B_1 = [\,b_1 \;\; b_1 \;\; b_1 \;\; b_1 \;\; \ldots\ldots \;\; N\,] \tag{4.10}$$

The prediction model for deriving PM2.5 [Step VII] is given by eqn. 4.11.

$$PM2.5_n = b_2 + LW_2 * logsig(B_1 + LW_1 * x_n) \tag{4.11}$$

Where, $PM2.5_n$ is normalized output. The input matrix x_n is formed using normalized values of CO, NO_2, SO_2 and VOC and the size of x_n is R×N where R=8 is the number of inputs and N=1838 is the number of values for each input. Eqn. 4.11 shows the usefulness of the approach to

obtain the value of PM2.5 based on CO, NO_2, SO_2 and VOC values only. Therefore, low cost sensors can be deployed with the derived model that offers opportunity to derive PM2.5 through signal processing algorithms. Eqn. 4.12 shows conversion to the original value from the normalized one using eqn. 4.3, in which $Xmax$ and $Xmin$ are taken as per Fig. 4.14.

$$PM2.5 = \frac{(PM2.5_n + 1) * (180.052 - 2.228)}{2} + 2.228 \tag{4.12}$$

The proposed approach based on the above analytical equations, eliminate the need for proprietary tools such as MATLAB. It can be obtained using any low cost processing tool (e.g. excel sheet etc.). A screenshot of an example is shown in Fig. 4.16. In this example an input matrix x of size 8×1838 is taken. Eqn. 4.11 is computed as following.

a. First, x_n is obtained by computing (eqn. 4.2)

b. Multiplying the two matrices of LW_1 (eqn. 4.6) and x_n, product term $LW_1 {}^* x_n$ is obtained.

c. Matrix B_1, formed using eqn. 4.10 is added in the product term $LW_1 {}^* x_n$.

d. Hidden layer activation function (eqn. 4.4) is applied to find the output of the hidden layer.

e. Output of the hidden layer is multiplied by LW_2 (eqn. 4.7).

f. Then matrix b_2 from eqn. 4.9, is added.

Finally $PM2.5_n$ (marked as Ⓐ in Fig. 4.16) is obtained by computing eqn. 4.11, which is normalized value of PM2.5. PM2.5 in the original unit is obtained by processing eqn. 4.12 (marked as Ⓑ in Fig. 4.16). Predicted values of PM2.5 obtained from eqn. 4.12 (marked as Ⓑ in Fig. 4.16) are close to the actual values of PM2.5 (marked as Ⓒ in Fig. 4.16). In Fig. 4.16, large variation in the successive values of PM2.5 is because of random division of training and testing data. Interestingly these computations can

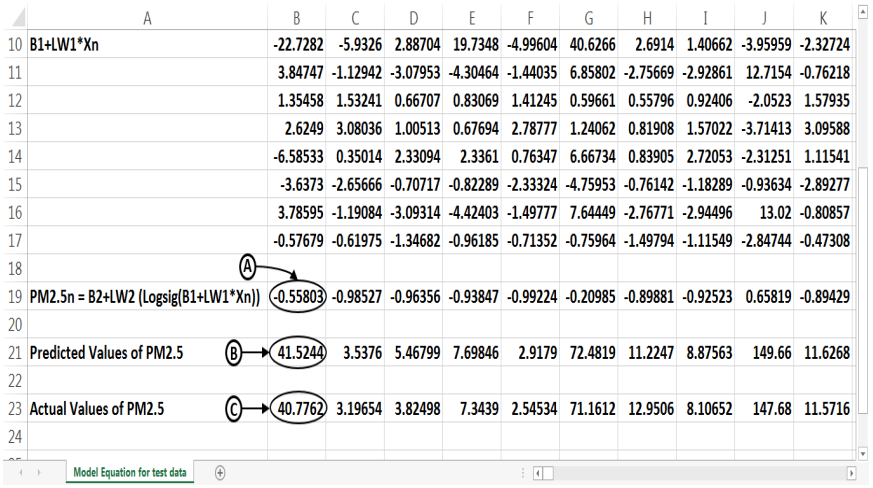

	A	B	C	D	E	F	G	H	I	J	K
10	B1+LW1*Xn	-22.7282	-5.9326	2.88704	19.7348	-4.99604	40.6266	2.6914	1.40662	-3.95959	-2.32724
11		3.84747	-1.12942	-3.07953	-4.30464	-1.44035	6.85802	-2.75669	-2.92861	12.7154	-0.76218
12		1.35458	1.53241	0.66707	0.83069	1.41245	0.59661	0.55796	0.92406	-2.0523	1.57935
13		2.6249	3.08036	1.00513	0.67694	2.78777	1.24062	0.81908	1.57022	-3.71413	3.09588
14		-6.58533	0.35014	2.33094	2.3361	0.76347	6.66734	0.83905	2.72053	-2.31251	1.11541
15		-3.6373	-2.65666	-0.70717	-0.82289	-2.33324	-4.75953	-0.76142	-1.18289	-0.93634	-2.89277
16		3.78595	-1.19084	-3.09314	-4.42403	-1.49777	7.64449	-2.76771	-2.94496	13.02	-0.80857
17		-0.57679	-0.61975	-1.34682	-0.96185	-0.71352	-0.75964	-1.49794	-1.11549	-2.84744	-0.47308
18		(A)									
19	PM2.5n = B2+LW2 (Logsig(B1+LW1*Xn))	-0.55803	-0.98527	-0.96356	-0.93847	-0.99224	-0.20985	-0.89881	-0.92523	0.65819	-0.89429
20											
21	Predicted Values of PM2.5 (B)	41.5244	3.5376	5.46799	7.69846	2.9179	72.4819	11.2247	8.87563	149.66	11.6268
22											
23	Actual Values of PM2.5 (C)	40.7762	3.19654	3.82498	7.3439	2.54534	71.1612	12.9506	8.10652	147.68	11.5716
24											

Model Equation for test data

Figure 4.16: Excel Sheet Used for Processing Prediction Model Equation

be ported to a wireless sensor node having basic memory and computation capability and the algorithms can still perform reliably.

The deployment of the developed prediction model requires to consider the following limitations based on the location, available monitoring stations and available monitoring parameters as predictors.

- Air pollution varies from one location to another based on the few parameters like human activity, traffic condition, structure of urban area and weather condition. Based on the location, predictors and predictand values as well as their maximum and minimum limit will change. So, application of presented prediction model for another location needs model training, validation and testing again which provides new coefficients in terms of weights and biases for accurate prediction with lower RMSE.

- Application of prediction model to another location requires large set of authentic data for training which is sometimes difficult due to the limitation on the number of online environment monitoring stations. Due to few monitoring parameters, and delay in the availability of data; offline stations are less preferable than online stations.

- Online stations of CPCB monitors pollutants that are greater than the

offline stations. Concentration data for large set of pollutants is the basic requirement for correlation study or developing prediction model. Due to limitation on the online stations available in the city, data were used from only one online station for training, validation and testing in the proposed study. This can be expanded in future by taking data from multiple online stations of different cities.

4.2 Model Results

Initially, Support Vector Machine (SVM) is used but from the results, it is found that ANN shows better performance compared to SVM in terms of RMSE. Results of SVM are shown in Table 4.2. Results are shown for Gaussian kernel as having better performance. For SVM obtained RMSE is of 2.862 during training and 2.823 during testing. Results show that RMSE is higher for SVM compared to RMSE obtained using ANN shown in Table 4.3. Considering better performance and ease in converting ANN into analytical equations, ANN is selected for the prediction model.

Table 4.2: Performance of SVM

Identifiers	**RMSE**
Training	2.862
Testing for unseen data	2.823

Table 4.3: Performance of the Proposed Prediction Model

Identifiers	**RMSE**	$\mathbf{R^2}$
Training	1.5971	0.9987
Validation	1.6347	0.9986
Testing	1.5843	0.9988
Testing for unseen data	1.5121	0.9988

Table 4.3 shows the performance of the selected prediction model from approx 100 runs of pseudocode. RMSE is 1.60 after training and 1.51 during testing, while R^2 is close to 1, which proves the acceptability of the analytical equations. The actual values of PM2.5 are compared to predicted results by

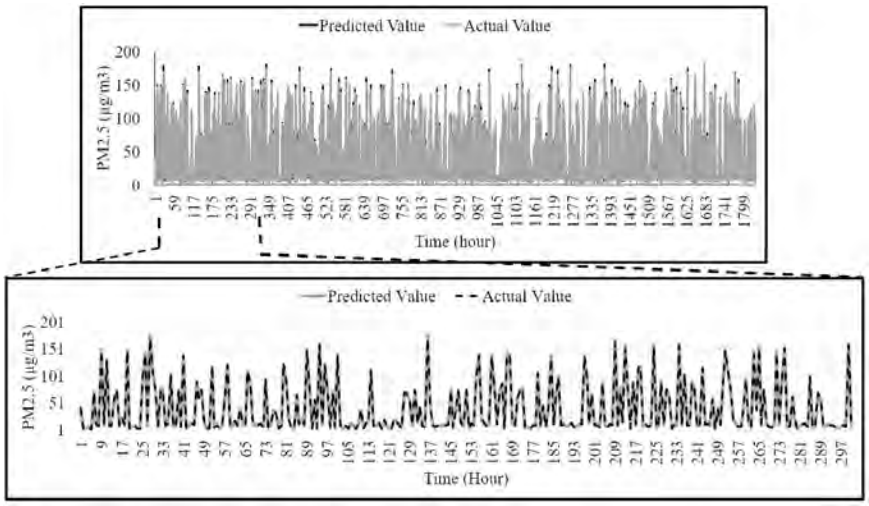

Figure 4.17: Good Match of the Results Obtained from Analytical Equation of Model with Actual Values

processing model (eqn. 4.12) in the excel sheet. The predicted results are very close to actual values as shown in Fig. 4.17. Closeness of predicted results with actual values shows accuracy and effectiveness of the proposed approach.

Previously developed prediction models, based on the past data of predictand, do not eliminate the need for costly, time consuming and bulky instruments. It is concluded that the proposed model reduces the number of inputs and ANN size compared to [36]. Results related to RMSE and R^2 of previous work are shown in Table 4.4. Using the proposed approach for prediction, RMSE and R^2 is better, compared to existing methods. RMSE of 1.7973µg/m^3 and R^2 of 0.9986 is obtained for the whole range of test data set which is equal to 1838 in this case. For reduced test data set of equal to 10, RMSE obtained is 146.10 µg/m^3 and R^2 is 0.9467. The proposed model presented in the form of analytical equations helps in implementation of a model using low cost wireless sensor node or processing tool.

The proposed prediction model is recalibrated in terms of the number of predictors, weights, and biases to show the effectiveness of the proposed approach. Instead of eight predictors, three predictors, CO, NO_2, and

Table 4.4: Summary of Previously Developed Prediction Models

Reference	**Predictand**	**RMSE**	**R^2**
[28]	O_3 (ppb)	0.30	0.69
[29]	O_3 (µg/m^3)	21.78	0.73
[30]	NO_2 (ppb)	7.3	0.91
[31]	NO_2 (µg/m^3)	13.93	0.93
[32]	PM 10 (µg/m^3)	12.16	0.83
[35]	PM 10 (µg/m^3)	11.656	0.983
[68]	PM2.5 (µg/m^3)	41.97	-
[69]	PM2.5 (µg/m^3)	12.8903	-
[70]	PM10 (µg/m^3)	18.4	0.895
[70]	PM2.5 (µg/m^3)	12.7	0.954
[74]	PM2.5 (µg/m^3)	6.777	0.99
[71]	PM2.5 (µg/m^3)	5.0324	0.79
[72]	PM2.5 (µg/m^3)	14.47	-
[73]	PM2.5 (µg/m^3)	24.06	-
[36]	BC (ng/m^3)	1480.746	0.586
This Work	PM2.5 (µg/m^3)	1.7973	0.9986

Benzene (VOC component) are taken considering availability of low cost sensors [80] which includes this type of multiple sensing parameters. The proposed approach can work for any other three sensing parameters after recalibrating model. In recalibration, CPCB smoothed data for CO, NO_2, and Benzene (VOC component) are used as it is considered as golden standard data. For recalibration, ANN shown in Fig. 4.15 is used with the same training and testing dataset (of three parameters), but the size of the input layer and hidden layer is reduced to three. Extracted weights and biases are represented in eqn. (4.13) to eqn. (4.16). Performance results are shown in Table 4.5. Results show, during testing RMSE is 7.5372 µg/m^3 and R^2 is 0.9708.

$$LW_1 = \begin{bmatrix} 26.281 & 3.456 & -12.391 \\ 17.898 & -0.863 & 11.305 \\ -0.996 & -0.502 & -1.205 \end{bmatrix} \tag{4.13}$$

$$LW_2 = \begin{bmatrix} -1.008 & 1.379 & -1.665 \end{bmatrix} \tag{4.14}$$

$$b_1 = \begin{bmatrix} 9.934 \\ 21.939 \\ 1.101 \end{bmatrix} \tag{4.15}$$

$$b_2 = \begin{bmatrix} 0.689 \end{bmatrix} \tag{4.16}$$

Table 4.5: Performance of Prediction Model for Three Predictors

Performance of	**RMSE**	**R^2**
Training	7.9297	0.9678
Validation	8.0954	0.9679
Testing	8.0049	0.9672
Testing for unseen data	7.5372	0.9708

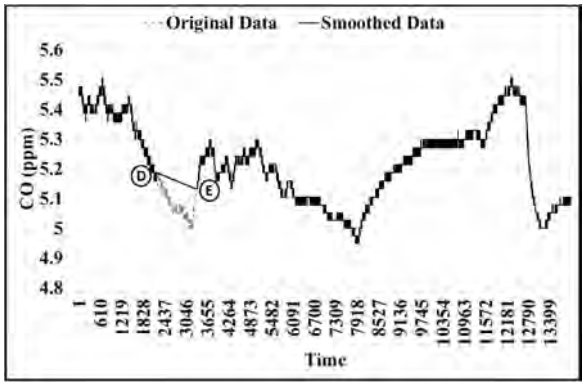

Figure 4.18: CO Data

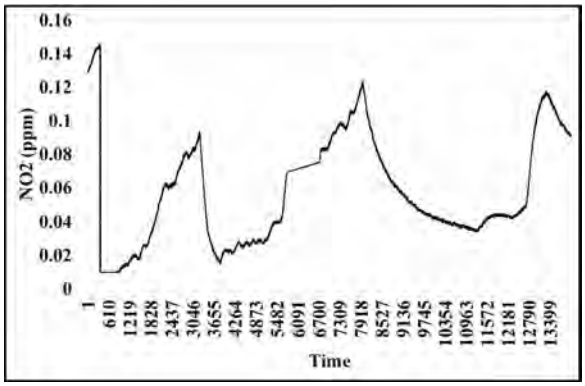

Figure 4.19: NO_2 Data

For testing the recalibrated model using WSN data, 14,000 samples of input predictors (CO, NO_2, and VOC) are obtained from mounted gas

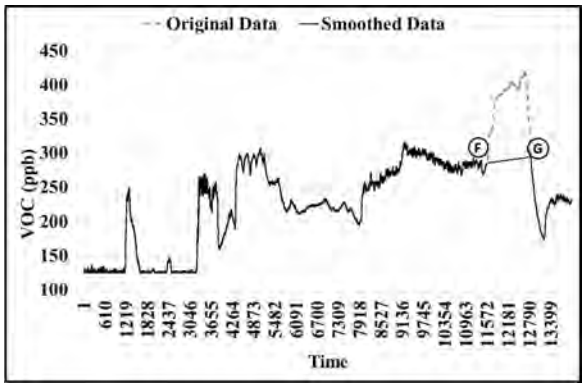

Figure 4.20: VOC Data

sensors. PM2.5 laser dust sensor (SEN0177) values are taken as a standard or actual values for evaluating the performance of the model. Fig. 4.18 to Fig. 4.20 show, input predictors; CO, NO_2, and VOC sensor data. Large variation at few points in obtained data is observed, which may be due to few reasons such as (i) due to lack of packaging of wireless sensor node (ii) due to malfunctioning of sensors for short duration (iii) due to the effect of environmental parameters on sensor values. As per the deployment location, sudden large change in the environment due to human activity or due to other parameters was not expected. Considering this factor it is required to remove the larger variation in the data before applying to the prediction model. For CO data, observing data before point Ⓓ and after point Ⓔ, an unusual negative peak is occurring between points Ⓓ and Ⓔ. So, this negative peak is smoothed out through the linear equation and the slope is obtained using y=mx equation. For NO_2, data is kept same as no larger outlier is observed. In VOC data, a large peak is observed between points Ⓕ and Ⓖ, which is exceeding the other data variations. So it is smoothed by a linear equation.

After smoothing, CO, NO_2 and VOC data are imported into excel sheet to compute prediction analytical eqn. (4.18) (as per eqn. (4.11)). The weights and biases obtained after recalibration as per eqn. (4.13) to eqn. (4.16) are used to compute eqn. (4.18). The matrix B_1 used in eqn. (4.18) is given by eqn. (4.17), where M is 14,000, which is equal to the total number of

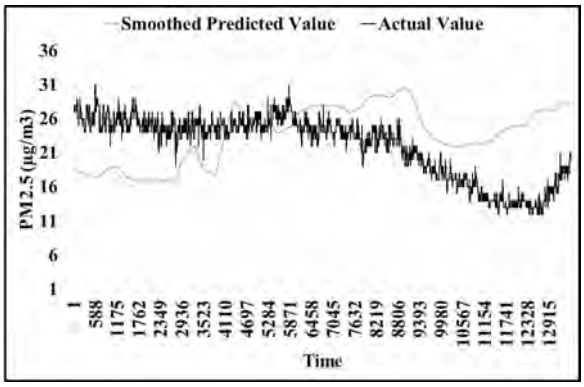

Figure 4.21: Smoothed Predicted and Actual Values of PM2.5

samples.

$$B_1 = \begin{bmatrix} b_1 & b_1 & b_1 & b_1 & . & . & . & . & . & M \end{bmatrix} \tag{4.17}$$

$$PM2.5_n = b_2 + LW_2 * logsig(B_1 + LW_1 * x_n) \tag{4.18}$$

$$PM2.5 = \frac{(PM2.5_n + 1) * (31 - 12)}{2} + 12 \tag{4.19}$$

eqn. (4.19), provides the final predicted output of PM2.5, in which 31 and 12 represent the maximum and minimum value of actual PM2.5. The predicted PM2.5 values obtained from eqn. (4.19) are smoothed out through a moving average filter with the window size of 500 data and after smoothing first 500 data are removed (see Fig. 4.21). From the results, it is observed that predicted values are following the actual values with minor variations. Performance in terms of RMSE, R^2, maximum absolute error and minimum absolute error is obtained as per Table 4.6. After smoothing the reduction is observed in maximum absolute error compared to other parameters. RMSE of 7.1269 µg/m^3 is obtained which is almost closer to RMSE of CPCB testing data shown in Table 4.6, while R^2 is less and equal to 0.05861. The lower value of R^2 is due to the fact that training data set used is obtained from the location, situated far away from the DA-IICT. The value of R^2 can be improved by training the model with a large

training dataset obtained from the monitoring station nearer to the place of deployment. The obtained results represent that for applying the developed model at new location requires large training data set (as a golden standard) nearer to the place of deployment for accurate results. Due to unavailability of monitoring station (hence larger training data set) nearer to the DA-IICT, it was difficult to improve the results with the same model.

Table 4.6: Testing Performance of Prediction Model for Three Predictors

Performance	**RMSE**	**R^2**	**Max Error**	**Min Error**
Without Smoothing	7.4024	0.06739	18.6722	-13.8190
With Smoothing	7.1269	0.05861	15.1823	-13.5660

4.3 Conclusion

In this Chapter, we have presented the analytical equations based prediction model for PM2.5. First, cross correlation study related to PM2.5 and other pollutants is done based on the standardized CPCB data. The developed prediction model of PM2.5 based on the correlation results is useful for online or offline measurements. The proposed approach based on analytical equations enables the use of any low cost processing tool and eliminates the need for costly propriety tool for simulation of model. Results obtained using this method with eight predictors and an excel sheet as a processing tool shows, RMSE of 1.7973µg/m^3 and R^2 0.9986 for a full range of test data set. A reduced data set provided an RMSE of 146.10 µg/m^3 and R^2 of 0.9467. The closeness of the results obtained through the proposed approach proves the effectiveness of the proposed approach. To show the effectiveness of the proposed approach, the derived prediction model was recalibrated with three predictors (CO, NO_2, and Benzene (VOC component) due to possibility of sensing all three parameters by one or two low cost sensors. The proposed approach can work for any other three sensing parameters too after recalibration. Testing results show RMSE of 7.5372 µg/m^3 and R^2 of 0.9708. The obtained results prove the effectiveness

of the proposed approach. The obtained results can be improved in future by recalibrating prediction model based on the data available from multiple stations located at the place of deployment. In comparison to existing methods, the proposed approach facilitates an efficient method that reduces overall computation cost. Furthermore, this model can be implemented on wireless sensor node for automated measurement of PM2.5. The proposed IoT enabled wireless sensor node discussed in Chapter 3 is useful for different applications. Detail about the deployment of the wireless sensor node for different applications is given in the following Chapter 5.

Chapter 5

Applications Scenario of IoT Sensor Node

In Chapter 3, we have discussed the development of IoT enabled wireless sensor node for environment monitoring. Proposed wireless sensor node can be used for multiple applications. At the initial phase of development, we have deployed the hardware at different places for validation of its working for different applications. This Chapter discusses the details and results about the deployment of developed wireless sensor node for different applications of indoor and outdoor environment such as (a) Museums (b) Smart Buildings and (c) Smart City.

The Chapter is organized as follows. In Section 5.1 we have discussed the detail about the deployment of the proposed wireless sensor node at Shreyas Folk Art Museum, Ahmedabad, India. The deployment results related to application of smart building are discussed in Section 5.2. Section 5.3 provides the results related to deployment of the proposed system for environment monitoring of Gandhinagar city, Gujarat, India. The selected deployment places helps in validation of the system for actual indoor and outdoor environment.

5.1 Museums

For museum curators, monitoring parameters like temperature, humidity and light is a major area of concern for preservation of artworks and artefacts. Variations in these parameters affect the life and preservation of the artwork, which gives rise to the need to continuously monitor these parameters. Accurate manual measurement and monitoring of these parameters is tedious, time consuming, unreliable and, to some degree, impossible. To achieve this a wireless sensor node is required to collect and monitor the data wirelessly. The proposed environment monitoring system is one possible solution to address these issues. To the best of authors knowledge, this is the first attempt to study an Indian Heritage building within the context of IoT.

There have been numerous efforts on microclimate monitoring using WSN. The work reported in the literature emphasizes the microclimate monitoring within the museum environment [91] for sensing parameters like temperature and humidity [92], [93]; occupancy in the museum for improving visitor experience [94], [95]; security and energy management [96] and the practical challenges during deployment [97].

Proposed system measures temperature, humidity and light which is essential to monitor the museum environment which, in turn, is important for preservation of the artwork in the museum. The work has been validated at Shreyas Folk Art Museum - an Indian Heritage site in Ahmedabad, India. A GUI that provides a graph for the parameters with continuous monitoring and recording of data is developed in LabVIEW. The recorded data is useful to museum curators for further analysis and can be useful for controlling the museum environment. Developed Android application proves useful for remote monitoring.

5.1.1 System Description

The proposed system consists of a transmitter node, repeater node and a sink node (receiver node) as shown in Fig. 5.1. The sensing platform supports one way communication from the transmitter to the receiver node

and can accommodate more repeater nodes, if required, to cover a larger area. Furthermore, the proposed system uses a custom hopping method for transmission over several nodes. This customized hopping method is simple and scalable. Finally, the data received at the sink node is transferred to a PC through a USB interface. The sensed data is depicted graphically and recorded in an excel sheet through a customized GUI, which is developed in LabVIEW. This data is then transmitted to the Android based smartphone, thereby enabling IoT.

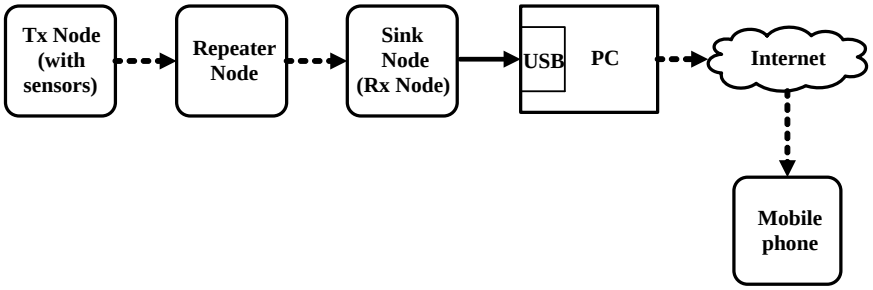

Figure 5.1: Proposed Deployment System

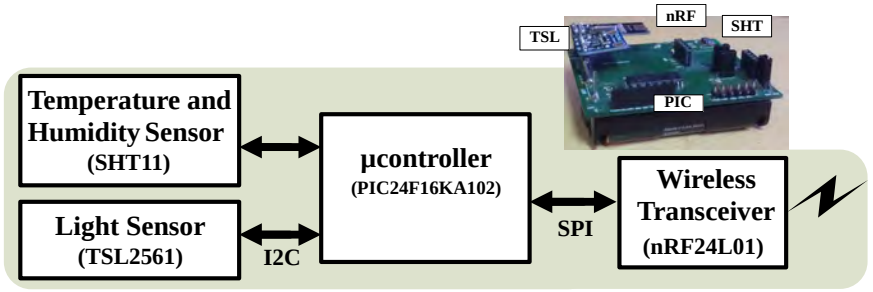

Figure 5.2: Proposed Wireless Sensor Node

5.1.2 Wireless Sensor Node

The proposed wireless sensor node consists of a temperature and humidity sensor, a light sensor, an ultra low power microcontroller and a wireless transceiver as shown in Fig. 5.2. The temperature, humidity and light readings are processed by the μcontroller and transmitted through the wireless transceiver. The repeater and receiver nodes have the same

components except the on-board sensors. Data sensing and aggregation on the node can be configured by customized software code and is dependent on the application. Further to this, a custom voting algorithm is implemented to increase data reliability. This algorithm reduces ambiguity in data up to a certain extent and is discussed in detail in the results Section. Power is supplied to the wireless sensor node and repeater node by two AA batteries, while the receiver node attached to a PC is powered through the USB interface.

The transceiver nRF24L01 can be configured to receive data from as many as the six different transmitters through as many as six different data pipes, each having its own unique address. In the proposed system only two data pipes are sufficient, i.e., pipe-0 for transmission between transmitter and repeater node and pipe-1 between repeater and receiver node.

The above selected μcontroller, transceiver and sensors provide an added advantage of operating all of them at a single voltage (3.0V), without the need for an expensive DC-DC conversion.

The operation of the wireless sensor node consists of two phases; (i) sensing and (ii) transmission. Table 5.1 shows the different states of the individual components. The bottom most row of the table shows the duration of time for which the modules are active in those states. For example, in state S1, the microcontroller is active for 1 *ms*, whereas all other modules (nRF24L01, SHT11, TSL2561) are in sleep state. The graphical representation of the states is also shown in Fig. 5.3, depicting the time duration and current consumption of the sensor node in different states. This provides an intuitive representation to optimize the operation of the sensor node depending upon the power requirement of the application.

5.1.3 Methodology for Sensing and Transmission

Initially, switching on the power automatically puts the transmitter node in state S1, where it stays for 1 *ms*. The node is programmed such that it immediately enters state S2. It remains in this state for 400 *ms* during which

Table 5.1: Duration of Different States of the Wireless Sensor Node

Modules/ States	**S1**	**S2**	**S3**	**S4**	**S5**	**S6**	**S7**	**S8**
μcontroller Transceiver SHT11 TSL2561	Active Standby Sleep Sleep	Active Standby Active Sleep	Active Standby Sleep Power Up	Active Standby Sleep Active	Active Standby Sleep Power Down	Active Standby Sleep Sleep	S2 to S6 repeated twice	Active Active Sleep Sleep
Time Duration	1 ms	400 ms	400 ms			1s		235 μs

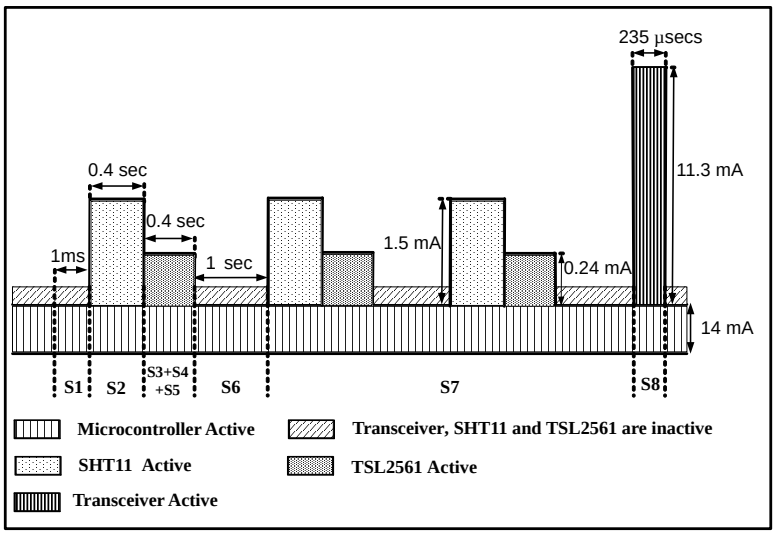

Figure 5.3: State Diagram for the Sensor Node

time, SHT11 is setup and data is written to the μcontroller memory. The duration of state S3 is also of 400 ms during which TSL2561 is setup, intensity data is measured and the sensor is switched to power down mode. After 1 *sec*, states S2 to S6 are repeated twice in state S7. In state S7, after the three sets of data are written to the μcontroller memory, a voting algorithm is performed to remove anomalies, if any. By doing so, the reliability of the data is enhanced and is shown in the results Section. Transceiver remains in standby mode for states S1 to S7 and after that in state S8 it becomes active and data is transmitted.

The transmission methodology is shown in Fig. 5.4. The data at sensor node is sent at every 5.4 *secs*. For convenience and reliability, the duration

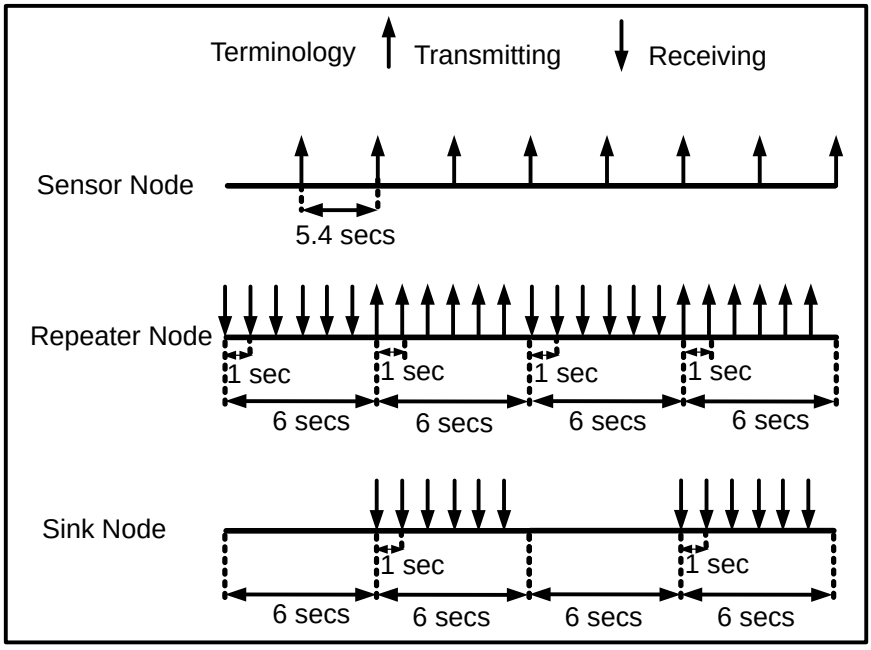

Figure 5.4: Transmission Methodology

of the reception at repeater node for a single transmission is set, a little bit longer than the 5.4 *secs*. At the receiver node, after the delay of 6 *secs*, data is received for 6 *secs* at the interval of 1 *sec*. The double hopping algorithm ensures that the receiver chooses the right data packet from the number of received data packets and thereby increases the reliability of the system.

However, reliability is increased at slightly higher power consumption as discussed in the experimental results. Furthermore, with the above sensing and transmission scheme, it is possible to quantify, in terms of power and time, the various states of the wireless sensor node at ease. This provides a scope to further optimization for future deployments. For example, if S1 is stretched during the sleep mode, the average power consumption is lowered, thereby prolonging the battery life. This is also explained and quantified in the experimental results.

Table 5.2 shows the power calculations for the sensor node. For different states, total current is calculated by adding currents of all modules, according to their states as stated in Table 5.4. For each state, the final value of the time is obtained by multiplication of time and repetition of time. For example, for

Table 5.2: Power Calculation for the Sensor Node

Modules	**S1**	**S2**	**S3+S4+S5**	**S6**	**S8**
	Current (mA) for different states				
Microcontroller	14	14	14	14	14
Transceiver	32e-3*	32e-3	32e-3	32e-3	11.3*
SHT11	1e-5	1.5	1e-5	1e-5	1e-5
TSL2561	3.2e-3*	3.2e-3	0.24*	3.2e-3	3.2e-3
Total I (mA)	14.03	15.53	14.27	14.03	25.30
Time (*secs*)	1e-3	0.4	0.4	1	2.35e-4
Repetition of time	1	3	3	3	1
Voltage	3	3	3	3	3
Energy (mJ)	0.04	55.90	51.37	126.27	0.017
Total Energy (mJ) =			233.59		
Total Time *secs* =			5.40		
Average Power (mW) =			43.25		

*Estimated current

state S2, final value of time is 1.2 *secs* which is obtained by multiplication of 0.4 *secs* and 3. Energy for different states is calculated by multiplication of total current, voltage and final value of time. Total energy is the summation of energy of all the states of the node. Total time calculated by summation of final value of time for all states is 5.4 *secs*. The average power of the sensor node is calculated by dividing the total energy by the total time period, and the result obtained is $43.25mW$.

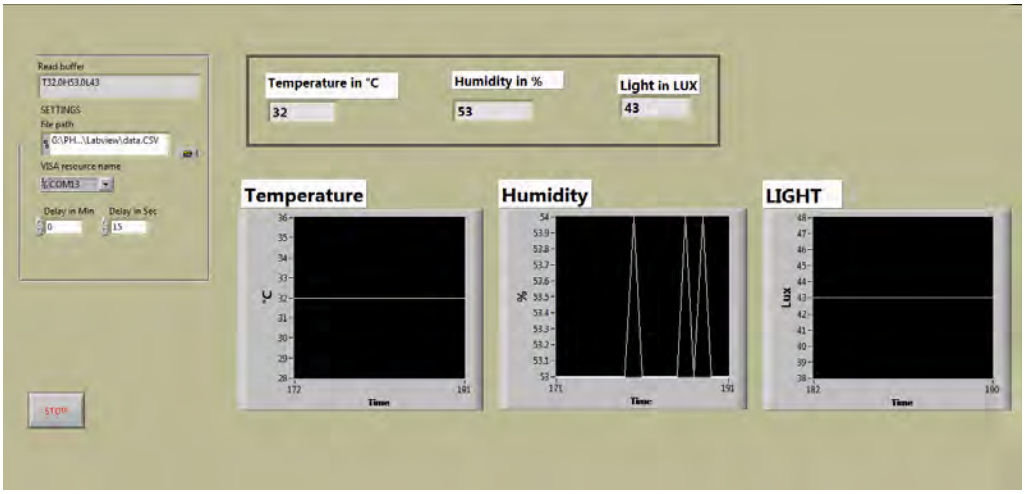

Figure 5.5: Graphical User Interface

5.1.4 Monitoring Platform

A graphical panel of GUI made in LabVIEW is developed as shown in Fig. 5.5. The monitored data is stored in excel sheet as shown in Fig. 5.6 with current date and time. In the front panel, the user can interrupt the setup and can configure the system setup. The programming is developed in such a way that the excel sheet stores the actual time of sensing instead of delayed time. Further, to enable IoT, the monitored data in LabVIEW is transferred to smartphone. Fig. 5.7 shows the screenshot of the developed Android application. The developed Android application is tested on a smartphone based on Android 4.3.

	A	B	C	D	E
1	Date	Time	Temperature	Humidity	Light
2	14-10-2015	09:20:11	32	51	43
3	14-10-2015	09:20:26	32	51	43
4	14-10-2015	09:20:41	32	51	43
5	14-10-2015	09:20:56	32	51	43

Figure 5.6: Excel Sheet Format for Data Storage

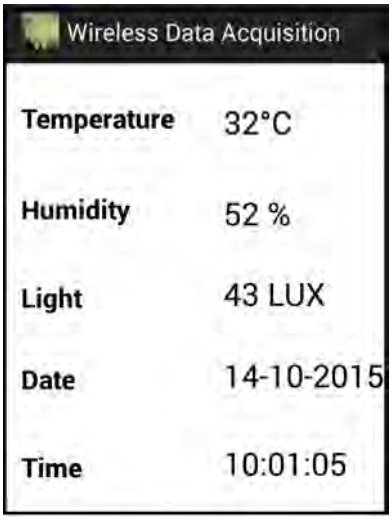

Figure 5.7: Android Application

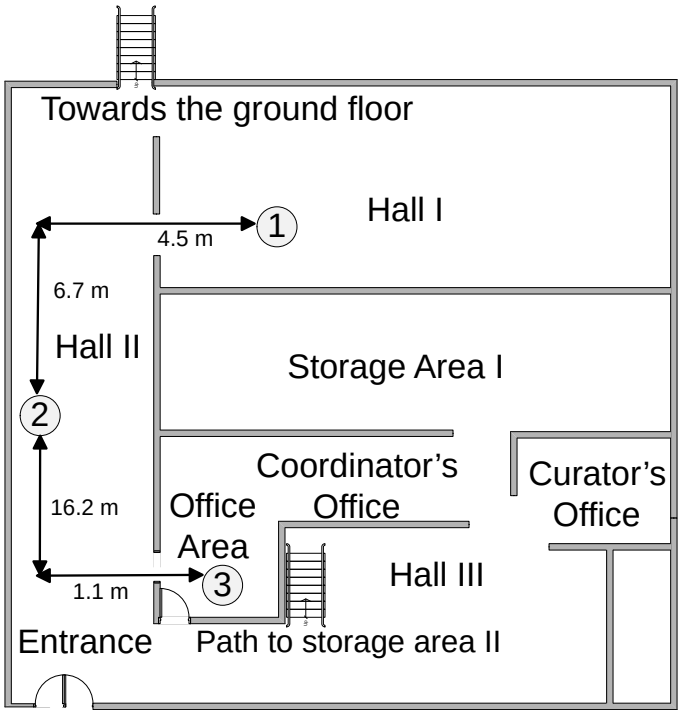

Figure 5.8: Floor Plan of the Museum

5.1.5 Experimental Results and Deployment

For the calibration of light sensor, in ten different light intensity environments, ten different results for the TSL2561 sensor are logged and ten results of lux meter from Metravi-1330 are manually recorded. Considering lux meter reading as a true value, obtained minimum and maximum value of relative error are 1.74% and 10.68% respectively. So it can be considered that TSL2561 readings are in close agreement with the actual values.

The developed system of double hopping is validated at Shreyas Folk Art Museum, Ahmedabad, India. The museum is of two floors, but the system is validated on the first floor because most of the artefacts are placed there. Considering light constraint for preservation of artefacts, intensity of the light is kept minimum during deployment in the museum. Fig. 5.8 shows the floor plan of the first floor of the museum and the deployment, in which ① represents sensor node, ② represents the repeater node and ③ is the sink

node. The proposed system is deployed in such a way that it covers major area of the museum. Results related to temperature, humidity and light for the deployment are shown in Fig. 5.9. Temperature variation is between 31.5 °C to 31.6 °C and relative humidity variation is between 68.4 % to 70.4 %. Light intensity results show light of 4 lux with some anomalies and can be reduced by a voting algorithm at the receiver node and is left as future work.

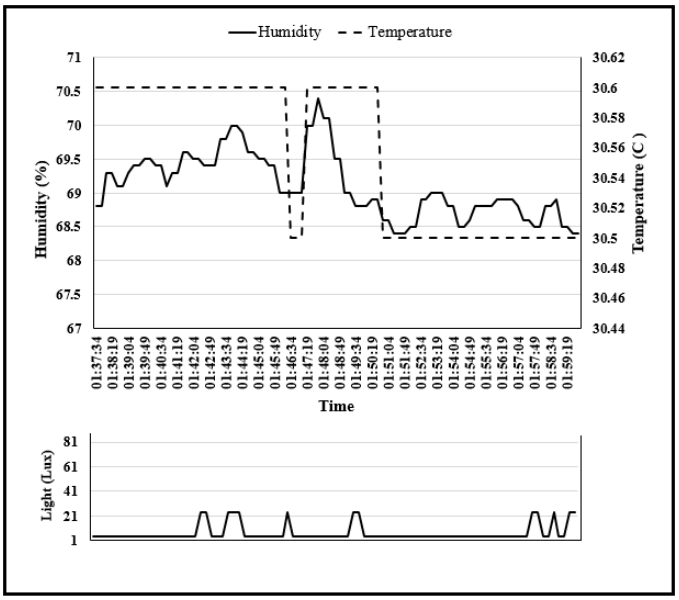

Figure 5.9: Temperature, Humidity and Light Results for the Deployment in Museum

5.2 Smart Buildings

One of the applications of IoT in the urban context is the smart building that promises to improve the quality of lifestyle of the residents by the use of Information and Communications Technology. The services for which quality can be enhanced in a smart building are (i) air quality management for reduction of pollution and healthy environment [56] and (ii) automation of public buildings for reducing human effort and energy consumption [46].

There have been numerous efforts on microclimate monitoring using WSN. In [45, 46, 56, 98] authors report indoor air quality monitoring by measuring pollution levels for indoor environments. In [99] developed a system which integrates IoT with home monitoring system. WSN based home monitoring system for determining wellness of elderly by monitoring their daily activities is also [100] implemented. A smart house off the shelf assistive technology for elderly and disabled people is presented in [101]. Work done in the area of smart homes based on different techniques and applications discussed in [102]. Middleware developed [103] for ambient intelligence applications such as home automation. A WSN for smart home which gives information about user's activity based on everyday objects status is discussed in [104].

The proposed system discussed in the earlier Section 5.1 can be used for the development of smart building. The proposed system is validated at DA-IICT laboratory building. Deployment of the proposed system in the laboratory is done by placing the sensor node and router node in the same room (at a distance of 4.75m from each other) and sink node in another room (at a distance of 3.75m from router node) so that they are separated by walls to create conditions similar to actual situations in smart buildings.

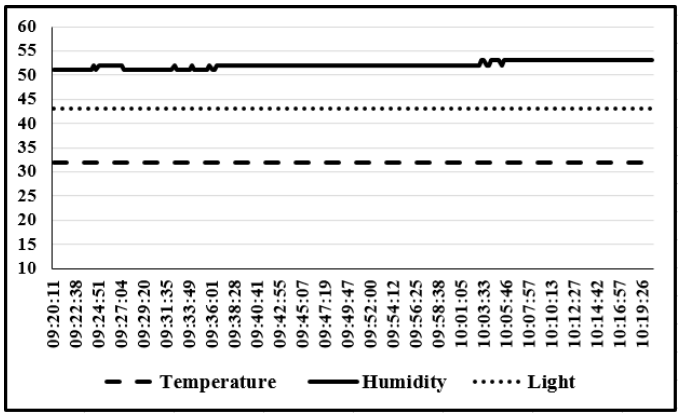

Figure 5.10: Temperature Humidity and Light Results

For this deployment, Fig. 5.10 shows the filtered results for the implemented IoT based monitoring system for one hour duration. In the results temperature is in Celsius, relative humidity is in % and light is in

Table 5.3: Reliability of Data Transmission

Time between two samples	**Expected Number of packets**	**Number of correctly received packets**	**Reliability(%)**
12 *secs*	1000	996	99.6

lux. With the same deployment reliability of the data, transmission is checked by recording data in excel sheet. From the results shown in Table 5.3, reliability obtained is 99.6%.

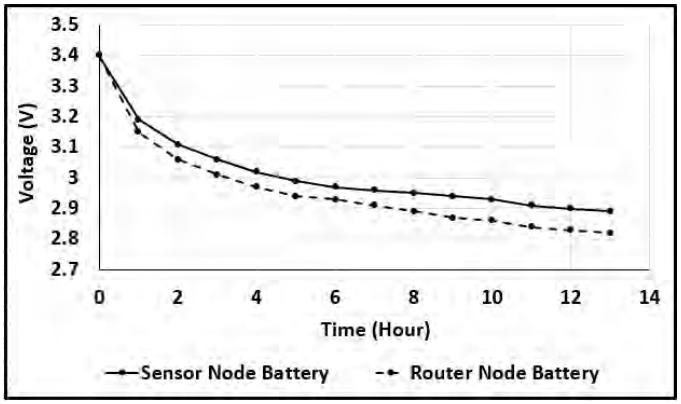

Figure 5.11: Measurements Results of the Wireless Sensor Node and Repeater Node Battery Voltage Over Time

Battery voltage of the sensor node and repeater node are measured using a multimeter at intervals of one hour over a period of thirteen hours. As shown in Fig. 5.11 the battery voltage drop out is high initially and then after a particular duration, it is 0.01V for each hour, with as occasional reading of 0.02V in some hours. Observing the initial dropout and final voltage of the battery over a period of thirteen hours shows that the battery dropout voltage of the router node is higher than that of the transmitter node. Higher power consumption of the repeater node is because of the methodology used for transmission, for getting higher reliability. After thirteen hours, battery voltage of the sensor node reaches 2.89V. With this drop of 0.51V in 13 hours, the battery discharging 1200mAh has an energy consumption of 7956 *mJ*. To calculate the estimated lifetime of the node, the total voltage drop is

taken to be 0.7V, at which the node stops functioning reliably. The energy consumption of the transmitter node at 0.7V with 1200mAh when divided with the average power consumption (Table 5.2), gives the estimated lifetime of the sensor node and is roughly about 20 hours. Based on the estimation and the state diagram (Fig. 5.3), by increasing the duration of the state S1, the battery life can be prolonged.

5.3 Smart City

One of the applications of IoT in the urban context is the smart city that promises to improve the quality and performance of urban services by the use of Information and Communications Technology (ICT). It also improves the lifestyle of the citizens by providing better facilities and simultaneously reduces the administrative efforts for management of the city and enabling effective utilization of resources and better quality of services to the citizens. The services for which quality can be enhanced in a smart city are monitoring the strength of buildings, waste management, air quality management, weather monitoring, noise monitoring, traffic management, parking management, energy consumption management and automation buildings. To provide services such as air quality management, weather monitoring and automation of homes and buildings in a smart city, the basic parameters are temperature, humidity and CO_2. To achieve this a wireless sensor node is required to collect and monitor the data wirelessly.

There have been numerous efforts on microclimate monitoring using WSN. The initial efforts of using ICT based technology for microclimate monitoring system that monitors parameters like temperature and humidity on a mobile device is discussed in [42, 43]. The deployment and networking and routing issues for similar microclimate monitoring systems are discussed in [105]. More recently, in [106], authors discuss the importance of technologies and architecture for urban IoT and a proof of concept monitoring system for a smart city. This Section discusses our efforts to develop a customized IoT enabled environment monitoring system to monitor important parameters such as temperature, humidity and CO_2. To

the best of our knowledge, this is the first effort to monitor environmental parameters within one of the smart cities in Gandhinagar, Gujarat, India.

5.3.1 System Description

The proposed IoT enabled sensing and monitoring system consists of a transmitter node (TX node) and receiver node (RX node) as shown in Fig. 5.12. The sensed data from the TX node is transmitted to RX node through wireless communication. Finally, the data received at the RX node is transferred to a PC) through a USB interface. The sensed data is depicted graphically and recorded in an excel sheet through a customized GUI, which is developed in LabVIEW. This data is then transmitted to a MySQL database via internet. The PHP API execution, on internet enables transfer of data from the MySQL database to the Android based smartphone, thereby enabling IoT based applications.

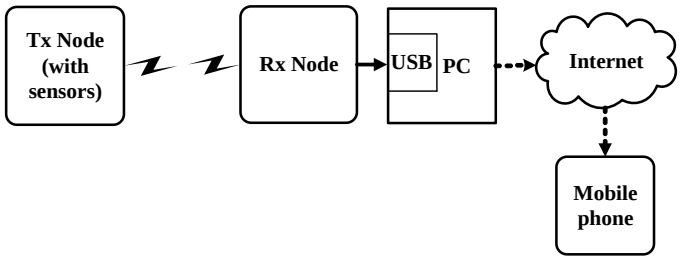

Figure 5.12: Architecture of the IoT Enabled Sensing and Monitoring System

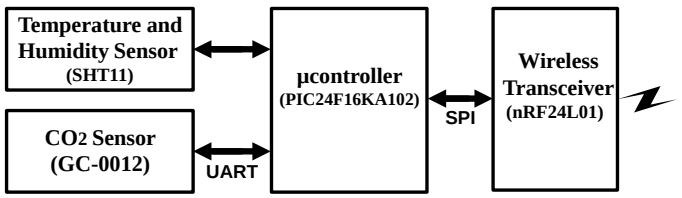

Figure 5.13: Proposed Sensor Node

5.3.2 Node

The proposed IoT enabled sensor node (wireless sensor node) consists of a temperature and humidity sensor, CO_2 sensor, an ultra low power

μcontroller and a wireless transceiver as shown in Fig. 5.13. The temperature, humidity and CO_2 readings are processed by the μcontroller and transmitted through the wireless transceiver. The receiver node has the same components except the onboard sensors. Data sensing and aggregation on the node can be configured by customized software code and is dependent on the application. Further to this, a custom voting algorithm is implemented at TX node for data reliability. Power is supplied to the TX node by three AA batteries, while the receiver node attached to a PC is powered through the USB interface.

The ultra low power COZIR^{TM} CO_2 sensor, GC-0012, from CO_2 Meter [107] is ideally suitable for the battery operated devices. Sensor works on Non-Dispersive Infrared (NDIR) absorption method, with measurement range of 0 to 10,000 ppm. Sensor has ultra low power consumption of 3.5 mW, with operating voltage range of 3.25 to 5.25 V.

Table 5.4: Duration of Different States of the Wireless Sensor Node

Modules/ States	**S1**	**S2**	**S3**	**S4**	**S5**	**S6**
μcontroller	Sleep	Active	Active	Active	S2 to S6	Active
Transceiver	Power Down	Power Down	Power Down	Power Down	repeated twice	Active
SHT11	Sleep	Active	Sleep	Sleep		Sleep
GC-0012	Sleep	Sleep	Active	Sleep		Sleep
Time Duration	34 *secs*	400 *ms*	0.11*secs*	1*sec*		235 μs

5.3.3 Methodology for Sensing and Transmission

The operation of the proposed wireless sensor node consists of three phases; (i) sleep (ii) sensing and (ii) transmission. Table 5.4 shows the different states of the individual components. The bottom most row of the table shows the duration of time for which the modules are active in those states. The graphical representation of the states is shown in Fig. 5.14, depicting the time duration and current consumption of the proposed wireless sensor node in different states.

Table 5.5: Power Calculation for the Proposed Wireless Sensor Node

Modules	**S1**	**S2**	**S3**	**S4**	**S6**
	Current (mA) for different states				
Microcontroller	5.4e-4	15.55	15.55	15.55	15.55
Transceiver	1.26e-3	1.26e-3	1.26e-3	1.26e-3	11.3
SHT11	1.3e-5	1.31	1.3e-5	1.3e-5	1.3e-5
GC-0012	-	-	0.68	-	-
Total I (mA)	1.8e-3	16.86	16.23	15.55	26.85
Time (*secs*)	34	0.4	0.11	1	2.35e-4
Repetition of time	1	3	3	2	1
Voltage	3.3	3.3	3.3	3.3	3.3
Energy (mJ)	0.20	66.77	17.67	102.63	0.02
Total Energy (mJ) =	187.29				
Total Time (sec) =	37.53				
Average Power (mW) =	4.99				

Initially, switching on the power automatically puts the wireless sensor node in state S1, where it stays for 34 *secs*. In state S1 all modules are in sleep state. After S1, it switches to state S2 of duration 0.4 *secs*, in which, SHT11 is setup and data is written to the μcontroller memory. Duration of S3 is 0.11 *secs*, in which GC-0012 is set up and data related to CO_2 is written in microcontroller memory. To keep the heating of SHT11 low, state S4 is kept of 1 *sec*. In state S5, states S2 to S3 are repeated twice at the interval of 1 *sec*. In state S5, after the three sets of data are written to the microcontroller memory, a voting algorithm is performed to remove anomalies, if any. In state S6, nRF24l01 is setup as a transmitter and data is sent to the receiver node. After state S6, S1 to S5 are repeated again. This provides an intuitive representation to optimize the operation of the proposed wireless sensor node depending upon the power requirement of the application. For example, enlarging S1 sufficiently will bring down the overall energy of the proposed wireless sensor node.

For transmission, it is assumed that data from the TX node is sent at every 37.53 *secs*. At the receiver node, after 39 *secs*, it is receiving data at regular intervals. Table 5.5 shows the power calculations for the proposed wireless sensor node. For different states, total current is calculated by adding

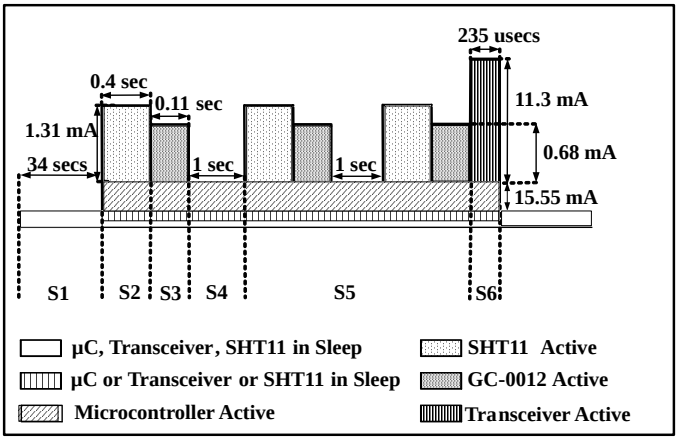

Figure 5.14: States (Sensing and Transmission) for the Proposed Wireless Sensor Node

currents of all modules, according to their states as stated in Fig. 5.14. For each state, the final value of the time is obtained by multiplication of time and repetition of time. For example, for state S2, final value of time is 0.4 *sec* is multiplied by 3. The total time calculated by summation of final value of time for all states is 37.53 *secs*. Energy for different states is calculated by multiplication of total current, voltage, time and repetition time. Total energy is the summation of energy of all the states of the proposed wireless sensor node. The average power is obtained by dividing the total energy (187.31mJ) with the total time period (37.53s) and is found to be 4.99 mW.

5.3.4 Monitoring Platform

A graphical panel of GUI made in LabVIEW is developed as shown in Fig. 5.15. The data is displayed in both graphical and numeric form and stored in excel sheet current date and time for further analysis. Fig. 5.16 shows the screenshot of the developed Android application. The developed Android application is tested on a smartphone based on Android 4.3.

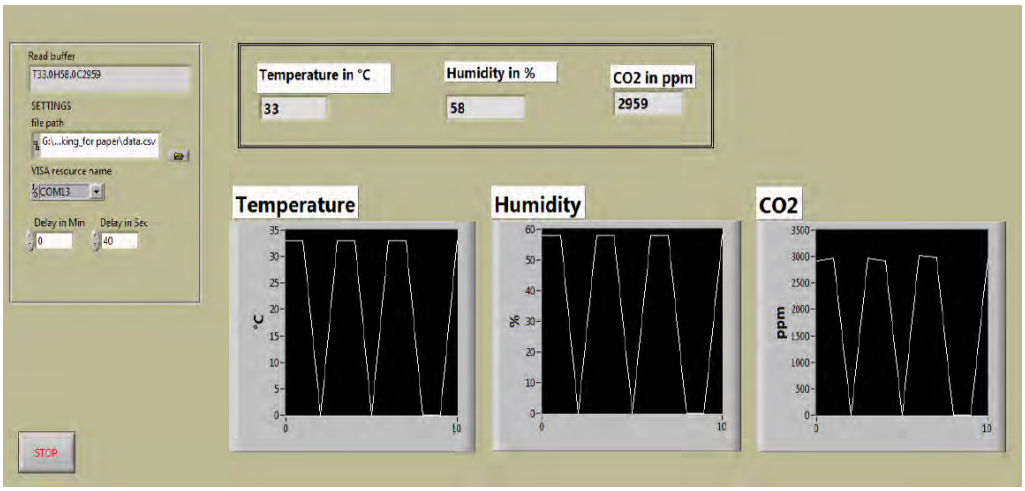

Figure 5.15: Graphical User Interface

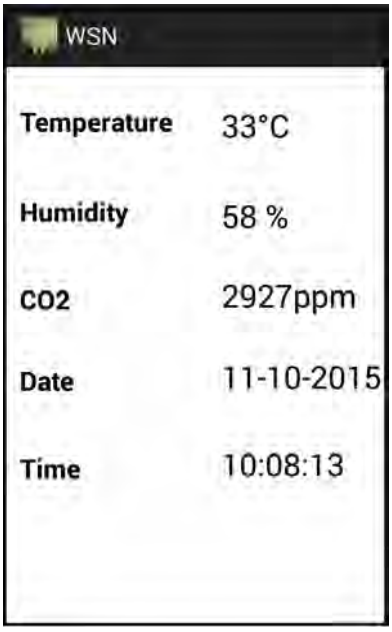

Figure 5.16: Android Application

5.3.5 Experimental Results and Deployment

To test the functionality of the proposed IoT enabled monitoring system, the proposed wireless sensor node was deployed at several places at the institute (DA-IICT) and around the city of Gandhinagar under varying conditions.

Fig. 5.17 shows the deployment of the proposed system at DA-IICT

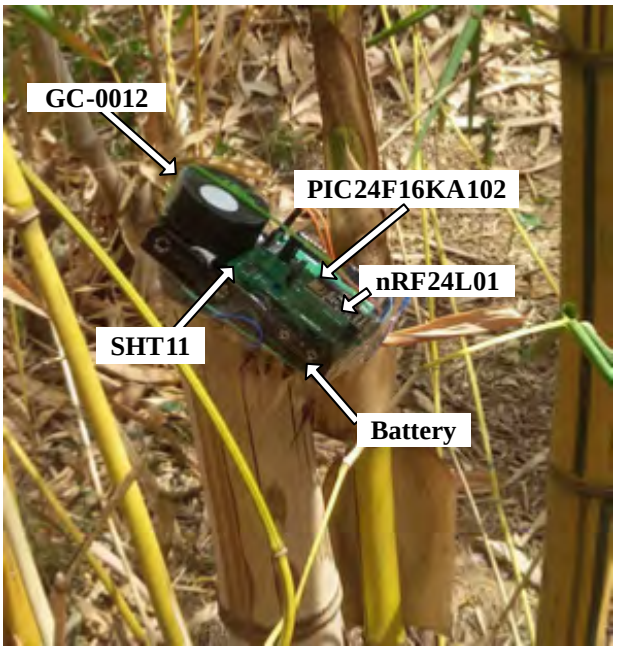

Figure 5.17: Deployment at DA-IICT

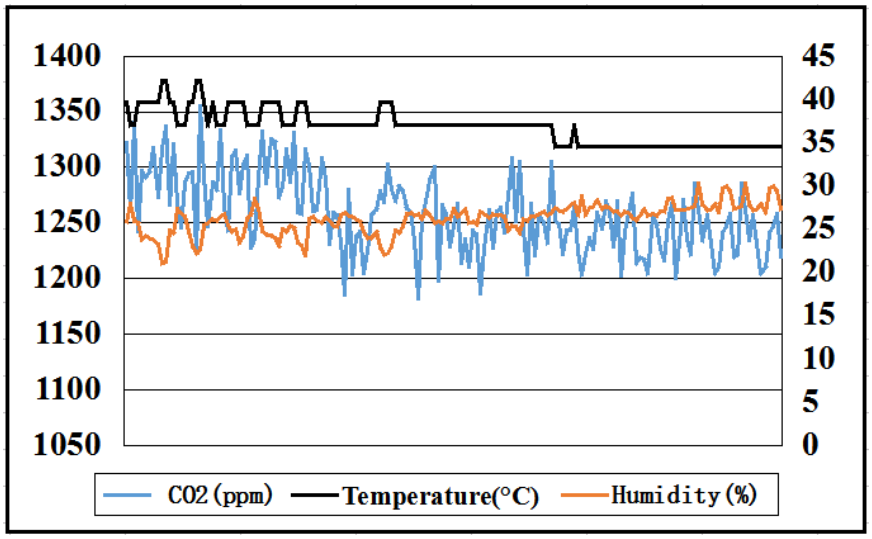

Figure 5.18: Results at DA-IICT

campus during April 2015. The transmitter node is placed near an office building (where monitoring was easier) and receiver node was kept at a distance of approximately 10 meters from the transmitter node.

Temperature, humidity and CO_2 concentration is monitored for five hours. Related results are shown in Fig. 5.18. As can be seen, temperature is seen to be varying between 34.5 °C to 42.2°C, humidity variation is between 21.1 % to 30.2 % and CO_2 concentration is varying between 1182 ppm to 1355 ppm.

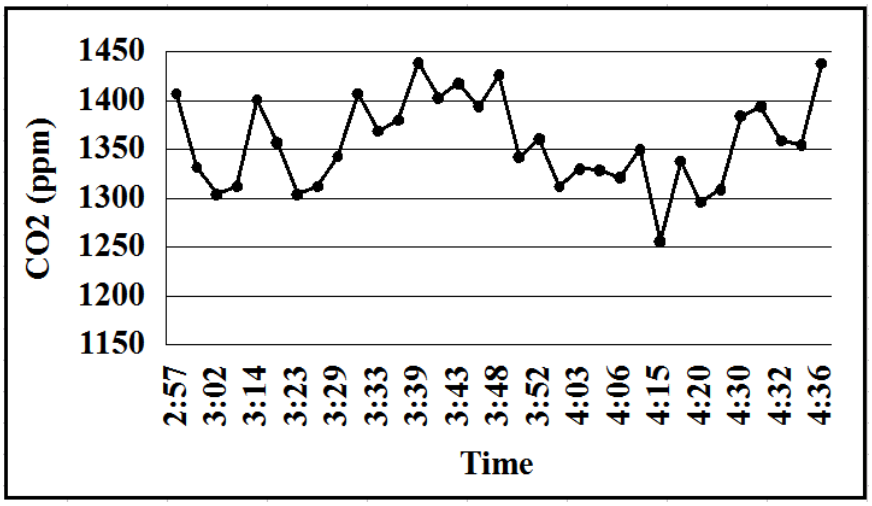

Figure 5.19: CO_2 Results for Gandhinagar, Gujarat, India

After a few iterations, the developed IoT enabled wireless sensor node was tested for the environmental conditions in the city of Gandhinagar, Gujarat, India during the same month. The proposed wireless sensor node was kept in the open (on top of a car) and readings were obtained for different areas at a distance of approximately 1 to 2 kms, which are likely to have variations in the CO_2 content. Data was monitored wirelessly through receiver connected to the PC (while on a moving car) and was recorded in an excel sheet through GUI made in LabVIEW for one and half hour. Results shown in Fig. 5.19, represents variation of CO_2, in the range of 1256 ppm to 1439 ppm, for different areas of the Gandhinagar (including the areas nearer to the smart buildings in GIFT city). These results were also available in the mobile device instantly; validating the proposed IoT enabled environmental monitoring system.

5.4 Conclusion

In this Chapter, we have presented the deployment results of the proposed wireless sensor node for different applications. The proposed wireless sensor node can be used for different applications after the replacement of sensor/supply. Proposed wireless sensor node for monitoring temperature, relative humidity and light with double hopping has been successfully implemented and validated at Shreyas Folk Art Museum, Ahmedabad and DA-IICT laboratory building. A high reliability of 99.6 % is obtained through a customized double hopping method. The average power consumption of the transmitter node is 43.25 mW. The wireless sensor node is also validated for the application of smart city at Gandhinagar, Gujarat, India, for monitoring temperature, relative humidity and CO2. Implemented sensor node has average power consumption of 4.99mW. Furthermore, the proposed wireless sensor node has an added advantage of remote access to the sensing data through an application that is tested on a smartphone based on Android 4.3. From the presented deployment results, working of the proposed wireless sensor node is validated for both indoor and outdoor environment.

Chapter 6

Conclusions and Future Research Directions

In this Chapter, we provide the conclusions by summarizing our main contributions in Section 6.1 followed by future research directions in Section 6.2.

6.1 Conclusions

In this thesis, we have presented the literature review related to different methods of environment monitoring and limitations of the classical methods used for it. We have proposed the architecture of the low power IoT enabled wireless sensing and monitoring system which store and monitor real time data of ten different parameters. In comparison with earlier research work, we have achieved low power consumption with more monitoring parameters. For the proposed system we have also tried to achieve high reliability of transmission through algorithms, accuracy of data trough calibration and remote monitoring and storage of data through IoT enabled monitoring platform. Achieved power consumption of the sensor node is $25.67mW$, which can be reduced further by prolonging the sleep time or sampling time of the sensor node. Estimated battery life is approximately 31 months for the measurement cycle of 60 *secs*. We have achieved the reliability of transmission as 97.4%. Developed IoT enabled

monitoring platform is successfully validated using personal computer and smartphone.

In our next work, we have presented analytical equations based prediction model for PM2.5. Cross correlation study related to PM2.5 and other pollutants is done based on the standardized CPCB data. Based on the correlation study, precursor gases (CO, NO_2, SO_2 and VOC) are selected to develop the prediction model of PM2.5. The proposed prediction model based on analytical equations can be processed using low cost processing tool and eliminates the need of power hungry sensor. Results show RMSE of 1.7973µg/m^3 and R^2 is 0.9986 for the whole range of test data set and for reduced data set of 10 obtained RMSE is 146.10 µg/m^3 and R^2 is 0.9467. The derived prediction model is also recalibrated with three predictors. For testing the recalibrated model, data of three predictors (CO, NO_2, VOC), are taken. Results show, RMSE of 7.5372 µg/m^3 and R^2 0.9708. The obtained results can be improved in future by recalibrating prediction model based on the data available from multiple stations at the place of deployment. The closeness of the results obtained through the proposed approach with actual values proves the effectiveness of the proposed approach. In comparison to time consuming conventional methods which are mostly useful for offline measurement, the proposed approach for prediction requires only the processing time for the equations, which reduces computational cost and applicable for offline and online measurement.

Proposed modular wireless sensor node is useful for different applications after the replacement of sensor and or supply. We have presented the deployment results of the proposed wireless sensor node for three different applications (a) Museums (b) Smart Building and (c) Smart City. The validation of the proposed system done at three different places (a) Shreyas Folk Art Museum, Ahmedabad, Gujarat, India (b) DA-IICT Laboratory Building, Gandhinagar, Gujarat, India and (c) Gandhinagar city, Gujarat, India, ensures the working of the system for indoor and outdoor applications.

6.2 Future Research Directions

In the process of this work, we have identified a few things that one may consider worth pursuing. These are briefly described as follows.

- Number of sensor nodes can be increased to cover the larger area for monitoring.
- AQI can be calculated and monitored based on the monitored pollutants.
- Number of monitored pollutants can be increased as per the AQI requirement.
- Auto calibration feature can be added by modification in hardware and software.
- Circuit for switching off the power supply of microcontroller can be explored for further power reduction.

Bibliography

[1] MOEF, "Epidemiological Study on Effect of Air Pollution on Human Health (Adults) in Delhi Ministry of Environment and Forests Epidemiological Study on Effect of Air Pollution on Human Health (Adults) in Delhi," no. July, 2012.

[2] W. H. Organization, *Health Effects of Particulate Matter*, [Online]. Available: http://www.euro.who.int/__data/assets/pdf_file/0006/189051/Health-effects-of-particulate-matter-final-Eng.pdf, (accessed on 4 March 2017).

[3] W. M. Hodan and W. R. Barnard, "Evaluating the Contribution of PM2.5 Precursor Gases and Re-Entrained Road Emissions to Mobile Source PM2.5 Particulate Matter Emissions," *MACTEC Federal Programs, Research Triangle Park, NC*, 2004.

[4] Central Pollution Control Board, *National Air Quality Monitoring Programme*, [Online]. Available: http://cpcb.nic.in/about-namp/, (accessed on 5 June 2017).

[5] Central Pollution Control Board, *National Air Quality Index*, [Online]. Available: http://www.indiaenvironmentportal.org.in/files/file/Air%20Quality%20Index.pdf, (accessed on 14 July 2017).

[6] Central Pollution Control Board, *How is AQI Calculated*, [Online]. Available: http://cpcb.nic.in/cpcbold/How_AQI_Calculated.pdf, (accessed on 24 August 2017).

[7] Central Pollution Control Board, *Guidelines for the Measurement of Ambient Air Pollutants Volume I*, [Online]. Available: http://indiaenvironmentportal.org.in/files/NAAQSManualVolumeI-1.pdf, (accessed on 14 August 2017).

[8] W. Y. Yi, K. M. Lo, T. Mak, K. S. Leung, Y. Leung, and M. L. Meng, "A Survey of Wireless Sensor Network Based Air Pollution Monitoring Systems," *Sensors*, vol. 15, no. 12, pp. 31 392–31 427, 2015.

[9] M. Budde, L. Zhang, and M. Beigl, "Distributed, Low-cost Particulate Matter Sensing: Scenarios, Challenges, Approaches," in *Proc. 1st Int. Conf. Atmospheric Dust*, 2014.

[10] Y. Ma, M. Richards, M. Ghanem, Y. Guo, and J. Hassard, "Air Pollution Monitoring and Mining Based on Sensor Grid in London," *Sensors*, vol. 8, no. 6, pp. 3601–3623, 2008.

[11] Central Pollution Control Board, "Indoor Air Pollution," [Online]. Available: http://www.indiaenvironmentportal.org.in/files/file/Draft%20Monitoring%20Protocol%20of%20Indoor%20Air%20Quality.pdf, (accessed on 14 August 2018).

[12] S. S. Amaral, J. A. de Carvalho, M. A. M. Costa, and C. Pinheiro, "An Overview of Particulate Matter Measurement Instruments," *Atmosphere*, vol. 6, no. 9, pp. 1327–1345, 2015.

[13] Central Pollution Control Board, *Guidelines for the Measurement of Ambient Air Pollutants Volume II*, [Online]. Available: http://www.indiaenvironmentportal.org.in/files/NAAQSManualVolumeII.pdf, (accessed on 14 August 2017).

[14] M. J. R. Vilcassim, G. D. Thurston, R. E. Peltier, and T. Gordon, "Black Carbon and Particulate Matter (PM2.5) Concentrations in New York City's Subway Stations," 2014.

[15] R. Gehrig and B. Buchmann, "Characterising Seasonal Variations and Spatial Distribution of Ambient PM10 and PM2.5 Concentrations

Based on Long-Term Swiss Monitoring Data," *Atmospheric Environment*, vol. 37, no. 19, pp. 2571–2580, 2003.

[16] A. Northcross, Z. Chowdhury, J. McCracken, E. Canuz, and K. R. Smith, "Estimating Personal PM2.5 Exposures Using CO Measurements in Guatemalan Households Cooking with Wood Fuel," *Journal of Environmental Monitoring*, vol. 12, no. 4, pp. 873–878, 2010.

[17] X. Querol, A. Alastuey, S. Rodriguez, F. Plana, E. Mantilla, and C. R. Ruiz, "Monitoring of PM10 and PM2.5 Around Primary Particulate Anthropogenic Emission Sources," *Atmospheric Environment*, vol. 35, no. 5, pp. 845–858, 2001.

[18] J. Hall, S. M. Loo, D. Stephenson, R. Butler, M. Pook, J. Kiepert, J. Anderson, and N. Terrell, "A Portable Wireless Particulate Sensor System for Continuous Real-Time Environmental Monitoring," in *42nd International Conference on Environmental Systems*, 2012, p. 3441.

[19] S. Mansour, N. Nasser, L. Karim, and A. Ali, "Wireless Sensor Network-Based Air Quality Monitoring System," in *Computing, Networking and Communications (ICNC), 2014 International Conference on*. IEEE, 2014, pp. 545–550.

[20] A. R. Kasar, D. S. Khemnar, N. P. Tembhurnikar *et al.*, "WSN Based Air Pollution Monitoring System," *International Journal of Science and Engineering Applications*, vol. 2, no. 4, pp. 55–59, 2013.

[21] J.-H. Liu, Y.-F. Chen, T.-S. Lin, D.-W. Lai, T.-H. Wen, C.-H. Sun, J.-Y. Juang, and J. A. Jiang, "Developed Urban Air Quality Monitoring System Based on Wireless Sensor Networks," in *2011 Fifth International Conference on Sensing Technology*, Nov 2011, pp. 549–554.

[22] Central Pollution Control Board, *Real Time Air Quality DataUpdated*, [Online]. Available: http://cpcb.nic.in/real-time-air-quality-data/, (accessed on 16 August 2017).

[23] Central Pollution Control Board. Monitoring Network. [Online]. Available: http://cpcb.nic.in/monitoring-network-3/, (accessed on 25 July 2017).

[24] D. Hasenfratz, O. Saukh, S. Sturzenegger, and L. Thiele, "Participatory Air Pollution Monitoring Using Smartphones," *Mobile Sensing*, vol. 1, pp. 1–5, 2012.

[25] M. Richards, M. Ghanem, M. Osmond, Y. Guo, and J. Hassard, "Grid-Based Analysis of Air Pollution Data," *Ecological Modelling*, vol. 194, no. 1, pp. 274–286, 2006.

[26] A. Peters, D. W. Dockery, J. E. Muller, and M. A. Mittleman, "Increased Particulate Air Pollution and the Triggering of Myocardial Infarction," *Circulation*, vol. 103, no. 23, pp. 2810–2815, 2001.

[27] O. Yu, L. Sheppard, T. Lumley, J. Q. Koenig, and G. G. Shapiro, "Effects of Ambient Air Pollution on Symptoms of Asthma in Seattle-Area Children Enrolled in the CAMP Study," *Environmental Health Perspectives*, vol. 108, no. 12, p. 1209, 2000.

[28] H.-C. Lu, J.-C. Hsieh, and T.-S. Chang, "Prediction of Daily Maximum Ozone Concentrations from Meteorological Conditions Using a Two-Stage Neural Network," *Atmospheric Research*, vol. 81, no. 2, pp. 124–139, 2006.

[29] S. I. V. Sousa, F. G. Martins, and M. C. Pereira, "Multiple Linear Regression and Artificial Neural Networks Based on Principal Components to Predict Ozone Concentrations," vol. 22, 2007.

[30] M. Gardner and S. Dorling, "Neural Network Modelling and Prediction of Hourly NO_x and NO_2 Concentrations in Urban Air in London," *Atmospheric Environment*, vol. 33, no. 5, pp. 709–719, 1999.

[31] A. B. Chelani and S. Devotta, "Air Quality Forecasting Using a Hybrid Autoregressive and Nonlinear Model," *Atmospheric Environment*, vol. 40, no. 10, pp. 1774–1780, 2006.

[32] G. Grivas and A. Chaloulakou, "Artificial Neural Network Models for Prediction of PM10 Hourly Concentrations, in the Greater Area of Athens, Greece," *Atmospheric Environment*, vol. 40, no. 7, pp. 1216–1229, 2006.

[33] H. Jef, M. Clemens, D. Gerwin, F. Frans, and B. Olivier, "A Neural Network Forecast for Daily Average PM10 Concentrations in Belgium," *Atmospheric Environment*, vol. 18, pp. 3279–3289, 2005.

[34] J. B. Ordieres, E. P. Vergara, R. S. Capuz, and R. E. Salazar, "Neural Network Prediction Model for Fine Particulate Matter (PM2.5) on the USe Mexico Border in´rez (Chihuahua) ElPaso (Texas) and Ciudad Jua," *Environmental Modelling and Software*, vol. 20, pp. 547–559, 2005.

[35] L. A. Díaz-Robles, J. C. Ortega, J. S. Fu, G. D. Reed, J. C. Chow, J. G. Watson, and J. A. Moncada-Herrera, "A Hybrid ARIMA and Artificial Neural Networks Model to Forecast Particulate Matter in Urban Areas: the Case of Temuco, Chile," *Atmospheric Environment*, vol. 42, no. 35, pp. 8331–8340, 2008.

[36] EveryAware, *Final Report on: Sensor Selection, Calibration and Testing; EveryAware Platform; Smartphone Applications*, [Online]. Available: http://www.everyaware.eu, (accessed on 14 August 2017).

[37] Environmental Protection Department of Hong Kong, *Air Quality Monitoring Equipment*, [Online]. Available: http://www.aqhi.gov.hk/en/monitoring-network/air-quality-monitoring-equipment.html, (accessed on 16 August 2017).

[38] S. Gokhale, *Air Pollution Sampling and Analysis Lab Manual*, 2009.

[39] M. Rossi and D. Brunelli, "Ultra Low Power CH4 Monitoring with Wireless Sensors," in *SENSORS, 2013 IEEE*. IEEE, 2013, pp. 1–4.

[40] P. Spachos and D. Hatzinakos, "Real-Time Indoor Carbon Dioxide Monitoring Through Cognitive Wireless Sensor Networks," *IEEE Sensors Journal*, vol. 16, no. 2, pp. 506–514, 2016.

[41] S. De Vito, P. Di Palma, C. Ambrosino, E. Massera, G. Burrasca, M. L. Miglietta, and G. Di Francia, "Wireless Sensor Networks for Distributed Chemical Sensing: Addressing Power Consumption Limits with On-Board Intelligence," *IEEE Sensors Journal*, vol. 11, no. 4, pp. 947–955, 2011.

[42] M. Ito, Y. Katagiri, M. Ishikawa, and H. Tokuda, "Airy Notes: An Experiment of Microclimate Monitoring in Shinjuku Gyoen Garden," *4th International Conference on Networked Sensing Systems, INSS*, pp. 260–266, 2007.

[43] S. Aram, A. Troiano, and E. Pasero, "Environment Sensing Using Smartphone," *2012 IEEE Sensors Applications Symposium, SAS 2012 - Proceedings*, pp. 110–113, 2012.

[44] A. Kumar, I. P. Singh, and S. K. Sud, "Energy Efficient and Low-Cost Indoor Environment Monitoring System Based on the IEEE 1451 Standard," *IEEE Sensors Journal*, vol. 11, no. 10, pp. 2598–2610, oct 2011.

[45] P. Changhai, Q. Kun, and W. Chenyang, "Design and Application of a VOC-Monitoring System Based on a ZigBee Wireless Sensor Network," *IEEE Sensors Journal*, vol. 15, no. 4, pp. 2255–2268, 2015.

[46] D. Brunelli, I. Minakov, R. Passerone, and M. Rossi, "POVOMON:An Ad-hoc Wireless Sensor Network for Indoor Environmental Monitoring," *2014 IEEE Workshop on Environmental, Energy, and Structural Monitoring Systems Proceedings*, pp. 1–6, 2014.

[47] N. Kularatna and B. Sudantha, "An Environmental Air Pollution Monitoring System Based on the IEEE 1451 Standard for Low Cost Requirements," *IEEE Sensors Journal*, vol. 8, no. 4, pp. 415–422, 2008.

[48] O. A. Postolache, J. D. Pereira, and P. S. Girao, "Smart Sensors Network for Air Quality Monitoring Applications," *IEEE Transactions on Instrumentation and Measurement*, vol. 58, no. 9, pp. 3253–3262, 2009.

[49] Jen-Hao Liu, Yu-Fan Chen, Tzu-Shiang Lin, Da-Wei Lai, Tzai-Hung Wen, Chih-Hong Sun, Jehn-Yih Juang, and J.-A. Jiang, "Developed Urban Air Quality Monitoring System Based on Wireless Sensor Networks," *2011 Fifth International Conference on Sensing Technology*, pp. 549–554, 2011.

[50] J. Hall, S. M. Loo, D. Stephenson, R. Butler, M. Pook, J. Kiepert, J. Anderson, and N. Terrell, "A Portable Wireless Particulate Sensor System for Continuous Real-Time Environmental Monitoring," *AIAA 42nd International Conference on Environmental Sensing*, no. July, pp. 1–14, 2012.

[51] A. R. Kasar, "WSN Based Air Pollution Monitoring System," vol. 2, no. 4, pp. 55–59, 2013.

[52] V. Jelicic, M. Magno, D. Brunelli, G. Paci, and L. Benini, "Context-Adaptive Multimodal Wireless Sensor Network for Energy-Efficient Gas Monitoring," *IEEE Sensors Journal*, vol. 13, no. 1, pp. 328–338, 2013.

[53] A. Kumar and G. P. Hancke, "Energy Efficient Environment Monitoring System Based on the IEEE 802.15.4 Standard for Low Cost Requirements," *IEEE Sensors Journal*, vol. 14, no. 8, pp. 2557–2566, 2014.

[54] J.-Y. Kim, C.-H. Chu, and S.-M. Shin, "ISSAQ: An Integrated Sensing Systems for Real-Time Indoor Air Quality Monitoring," *IEEE Sensors Journal*, vol. 14, no. 12, pp. 4230–4244, 2014.

[55] S. Mansour, N. Nasser, L. Karim, and A. Ali, "Wireless Sensor Network Based Air Quality Monitoring System," *2014 International Conference*

on Computing, Networking and Communications (ICNC), pp. 545–550, 2014.

[56] S. C. Folea and G. Mois, "A Low-Power Wireless Sensor for Online Ambient Monitoring," *IEEE Sensors Journal*, vol. 15, no. 2, pp. 742–749, 2015.

[57] A. Priyadarshini, N. Dehury, and A. K. Samantaray, "A Real Time Portable Embedded System Design for Particulate Matter Monitoring," *2015 IEEE Bombay Section Symposium: Frontiers of Technology: Fuelling Prosperity of Planet and People, IBSS 2015*, 2016.

[58] K. K. Khedo, R. Perseedoss, and A. Mungur, "A Wireless Sensor Network Air Pollution Monitoring System," *International Journal of Wireless and Mobile Networks*, 2010.

[59] K. Zheng, S. Zhao, Z. Yang, X. Xiong, and W. Xiang, "Design and Implementation of LPWA-Based Air Quality Monitoring System," *IEEE Access*, vol. 4, pp. 3238–3245, 2016.

[60] Nova Fitness Co., Ltd, *Laser PM2.5 Sensor Specifications*, [Online]. Available: https://cdn.sparkfun.com/assets/parts/1/2/2/7/5/SDS021_laser_PM2.5_sensor_specification-V1.0.pdf, (accessed on 18 August 2017).

[61] Aeroqual, *Particulate Matter Sensor PM10/PM2.5*, [Online]. Available: https://www.aeroqual.com/product/particulate-matter-sensor-pm10_pm2-5, (accessed on 18 August 2017).

[62] Libelium, *Particle Matter−Dust Sensor (PM1/PM2.5/PM10)*, [Online]. Available: http://www.libelium.com/particle-matter-dust-sensor-pm1-pm25-pm10-air-quality-smart-cities/, (accessed on 18 August 2017).

[63] D. Miller, "Precursor Effects on SO_2 Oxidation," *Atmospheric Environment (1967)*, vol. 12, no. 1-3, pp. 273–280, 1978.

[64] Commission on Natural Resources, National Academy of Sciences, National Academy of Engineering , National Research Council, *Air Quality and Stationary Source Emission Control*, [Online]. Available: https://www.nap.edu/read/10840/chapter/8, (accessed on 24 January 2018).

[65] V. A. Dutkiewicz, M. Das, and L. Husain, "The Relationship between Regional SO2 Emissions and Downwind Aerosol Sulfate Concentrations in The Northeastern US," *Atmospheric Environment*, vol. 34, no. 11, pp. 1821–1832, 2000.

[66] A. Gupta, R. Kumar, K. M. Kumari, and S. Srivastava, "Measurement of NO2, HNO3, NH3 and SO2 and Related Particulate Matter at a Rural Site in Rampur, India," *Atmospheric Environment*, vol. 37, no. 34, pp. 4837–4846, 2003.

[67] E. Robinson and R. C. Robbins, "Gaseous Nitrogen Compound Pollutants from Urban and Natural Sources," *Journal of the Air Pollution Control Association*, vol. 20, no. 5, pp. 303–306, 1970.

[68] Y. Chen, "Prediction Algorithm of PM2.5 Mass Concentration Based on Adaptive BP Neural Network," *Computing*, vol. 100, no. 8, pp. 825–838, 2018.

[69] D.-j. Liu and L. Li, "Application Study of Comprehensive Forecasting Model Based on Entropy Weighting Method on Trend of PM2.5 Concentration in Guangzhou, China," *International journal of environmental research and public health*, vol. 12, no. 6, pp. 7085–7099, 2015.

[70] M. Fu, W. Wang, Z. Le, and M. S. Khorram, "Prediction of Particular Matter Concentrations by Developed Feed-Forward Neural Network with Rolling Mechanism and Gray Model," *Neural Computing and Applications*, vol. 26, no. 8, pp. 1789–1797, 2015.

[71] S. Ausati and J. Amanollahi, "Assessing the Accuracy of ANFIS, EEMD-GRNN, PCR, and MLR Models in Predicting PM2.5," *Atmospheric Environment*, vol. 142, pp. 465–474, 2016.

[72] W. Sun and J. Sun, "Daily PM2.5 Concentration Prediction Based on Principal Component Analysis and LSSVM Optimized by Cuckoo Search Algorithm," *Journal of Environmental Management*, vol. 188, pp. 144–152, 2017.

[73] X. Ni, H. Huang, and W. Du, "Relevance Analysis and Short-Term Prediction of PM2.5 Concentrations in Beijing Based on Multi-Source Data," *Atmospheric Environment*, vol. 150, pp. 146–161, 2017.

[74] B. Chen, X. Wang, L. Yu, H. Wang, Y. Li, J. Chen, J. Zhu, H. Nan, and L. Hou, "Prediction of PM2.5 Concentration in a Agricultural Park Based on BP Artificial Neural Network," *Advance Journal of Food Science and Technology*, vol. 11, no. 4, pp. 274–280, 2016.

[75] J. Shah and B. Mishra, "IoT Enabled Environmental Monitoring System for Smart Cities," in *Internet of Things and Applications (IOTA), International Conference on.* IEEE, 2016, pp. 383–388.

[76] Sensirion, *SHT1x Datasheet*, [Online]. Available: http:/www.sensirion.com, (accessed on 4 June 2017).

[77] T. A. O. Solutions, *TSL2560,TSL2561,Light-To-Digital Converter*, [Online]. Available: http://www.taosinc.com, (accessed on 4 March 2017).

[78] B. Sensortec, *BMP180 Digital Pressure Sensor*, [Online]. Available: https://www.bosch-sensortec.com, (accessed on 4 January 2017).

[79] S. Sensortech, *The MiCS-VZ-86/89 is an Integrated Sensor Board for Indoor Air Quality Monitoring*, [Online]. Available: http://www.sgxsensortech.com, (accessed on 17 January 2017).

[80] SGX, *Data Sheet,The MiCS-6814 is a Compact MOS Sensor with Three Fully Independent Sensing Elements on One Package*, [Online]. Available: http://www.sgxsensortech.com, (accessed on 7 January 2017).

[81] Nordic Semiconductor, *Single Chip 2.4GHz Transciever nRF24L01*, [Online]. Available: http://www.nordicsemi.com, (accessed on 7 March 2018).

[82] J. Shah and B. Mishra, "Customized IoT Enabled Wireless Sensing and Monitoring Platform for Preservation of Artwork in Heritage Buildings," in *Wireless Communications, Signal Processing and Networking (WiSPNET), International Conference on*. IEEE, 2016, pp. 361–366.

[83] J. Shah and B. Mishra, "Customized IoT Enabled Wireless Sensing and Monitoring Platform for Smart Buildings," vol. 23. Procedia Technology, Elsevier, 2016, pp. 256–263.

[84] G. Grivas and A. Ã. Chaloulakou, "Artificial Neural Network Models for Prediction of PM10 Hourly Concentrations, in the Greater Area of Athens, Greece," vol. 40, pp. 1216–1229, 2006.

[85] A. Chaloulakou, M. Saisana, and N. Spyrellis, "Comparative Assessment of Neural Networks and Regression Models for Forecasting Summertime Ozone in Athens," *Science of the Total Environment*, vol. 313, no. 1-3, pp. 1–13, 2003.

[86] J. Kukkonen, L. Partanen, A. Karppinen, J. Ruuskanen, H. Junninen, M. Kolehmainen, H. Niska, S. Dorling, T. Chatterton, and R. Foxall, "Extensive Evaluation of Neural Network Models for the Prediction of NO_2 and PM10 Concentrations, Compared with a Deterministic Modelling System and Measurements in Central Helsinki," *Atmospheric Environment*, vol. 37, no. 32, pp. 4539–4550, 2003.

[87] Mathworks. Multilayer Neural Network Architecture. Available: http://www.mathworks.com/help/nnet/ug/multilayer-neural-network-architecture.html, (accessed on 25 August 2017).

[88] Mathbits. Correlation Cofficient. Available: https://mathbits.com/MathBits/TISection/Statistics2/correlation.htm,(accessed on 27 July 2017).

[89] B. Sharma and K. Venugopalan, "Comparison of Neural Network Training Functions for Hematoma Classification in Brain CT Images," *IOSR-JCE*, vol. 16, no. 1, pp. 31–5, 2014.

[90] The MathWorks Inc. Train and Apply Multilayer Neural Networks. Available: http://www.mathworks.com/help/nnet/ug/train-and-apply-multilayer-neural-networks.html, (accessed on 25 July 2017).

[91] "The Research on Applying RFID Information System Architecture for Museum Service," *ICCIT 2009 - 4th International Conference on Computer Sciences and Convergence Information Technology*, pp. 218–222, 2009.

[92] L. de Brito, L. Peralta, F. Santos, and R. Fernandes, "Wireless Sensor Networks Applied to Museums' Environmental Monitoring," in *Wireless and Mobile Communications, 2008. ICWMC '08. The Fourth International Conference on*, July 2008, pp. 364–369.

[93] G. Menduni, F. Viani, F. Robol, E. Giarola, a. Polo, G. Oliveri, P. Rocca, and a. Massa, "A WSN-Based Architecture for the E-Museum - The experience at 'Sala dei 500' in Palazzo Vecchio (Florence)," *IEEE Antennas and Propagation Society, AP-S International Symposium (Digest)*, pp. 1114–1115, 2013.

[94] S. Pai, P. Kuryloski, H. Yip, S. Yennamandra, S. Wicker, K. Boehner, and G. Gay, "Networks of Sensors in Public Spaces: Combining Technology with Art," *Proceedings - 21st International Conference on Advanced Information Networking and Applications Workshops/Symposia, AINAW'07*, vol. 1, pp. 396–402, 2007.

[95] F. Viani, A. Polo, F. Robol, G. Oliveri, P. Rocca, and A. Massa, "Crowd Detection and Occupancy Estimation Through Indirect Environmental Measurements," no. EuCAP, pp. 2546–2549, 2014.

[96] A. Corovic, L. Kadric, N. Lipa, S. Opanovic, and N. Nosovic, "eMuseum - More Interesting Way of Learning from the Past," *Mipro*, pp. 900–904, 2012.

[97] H. F. Wang, Q. Tian, Z. Z. Hu, and C. Lankun, "The Design of Wireless Micro-Environment Monitoring System," *Proceedings - International Conference on Electrical and Control Engineering, ICECE 2010*, no. 1, pp. 2324–2327, 2010.

[98] B. Mishra, C. Botteron, G. Tasselli, C. Robert, P. A. Farine, P. Janphuang, D. Briand, and N. F. de Rooij, "A Sub 100μW UWB Sensor-Node Powered by a Piezoelectric Vibration Harvester," in *Wireless Information Technology and Systems (ICWITS), 2012 IEEE International Conference on.* IEEE, 2012, pp. 1–4.

[99] S. D. T. Kelly, N. K. Suryadevara, and S. C. Mukhopadhyay, "Towards the Implementation of IoT for Environmental Condition Monitoring in Homes," *IEEE Sensors Journal*, vol. 13, no. 10, pp. 3846–3853, 2013.

[100] N. K. Suryadevara, S. Member, and S. C. Mukhopadhyay, "System for Wellness Determination of Elderly," *IEEE Sensor Journal*, vol. 12, no. 6, pp. 1965–1972, 2012.

[101] S. Helal, W. Mann, H. El-Zabadani, J. King, Y. Kaddoura, and E. Jansen, "The Gator Tech Smart House: A Programmable Pervasive Space," *Computer*, vol. 38, no. 3, pp. 50–60, 2005.

[102] L. C. De Silva, C. Morikawa, and I. M. Petra, "State of the Art of Smart Homes," *Engineering Applications of Artificial Intelligence*, vol. 25, no. 7, pp. 1313–1321, 2012.

[103] M. Eisenhauer, P. Rosengren, and P. Antolin, "A Development Platform for Integrating Wireless Devices and Sensors into Ambient

Intelligence Systems," *2009 6th IEEE Annual Communications Society Conference on Sensor, Mesh and Ad Hoc Communications and Networks Workshops, SECON Workshops 2009*, vol. 00, no. c, pp. 1–3, 2009.

[104] L. Olivier, "Designing a Smart Home Environment Using a Wireless Sensor Networking of Everyday Objects," pp. 189–194, 2008.

[105] F. Farahmand, P. Yu, J. Ou, and J. J. P. C. Rodrigues, "SoNET: A Delay-Tolerant Geo-Sensor Network for Environmental Monitoring," *2012 IEEE 10th International New Circuits and Systems Conference, NEWCAS 2012*, pp. 217–220, 2012.

[106] A. Zanella, S. Member, N. Bui, A. Castellani, L. Vangelista, and M. Zorzi, "Internet of Things for Smart Cities," *IEEE Internet of Things*, vol. 1, no. 1, pp. 22–32, 2014.

[107] CO2Meter, *COZIR^{TM} Ultra Low Power Carbon Dioxide Sensor*, [Online]. Available: http://www.co2meter.com/products/cozir-0-2-co2-sensor, (accessed on 21 March 2017).

List of Publications

International Conference Proceedings

- Shah, Jalpa and Mishra, Biswajit, "IoT enabled environmental monitoring system for smart cities." in *International Conference on In Internet of Things and Applications (IOTA)*, IEEE, 2016, pp. 383-388.
- Shah, Jalpa and Mishra, Biswajit, "Customized IoT enabled Wireless Sensing and Monitoring Platform for preservation of artwork in heritage buildings" in *International Conference on Wireless Communications, Signal Processing and Networking (WiSPNET)*, IEEE, 2016, pp. 361–366.
- Shah, Jalpa and Mishra, Biswajit, "Customized IoT enabled Wireless Sensing and Monitoring Platform for Smart Buildings" in *Procedia Technology*, Elsevier, 2016, vol. 23, pp. 256–263.

Journal

- Jalpa Shah and Biswajit Mishra, "IoT Enabled Low Power Environment Monitoring System for Prediction of PM2.5 " Pervasive and Mobile Computing, Elsevier (Under review).
- Jalpa Shah and Biswajit Mishra, "Analytical Equations based Prediction Approach for PM2.5 using Artificial Neural Network" Neural Computing and Applications, Springer (Under review).